CERTIFICATE OF MAILING BY FIRST CLASS MAIL

I hereby certify that this correspondence is being deposited with the United States Postal Service as first class mail in an envelope addressed to the Commissioner for Patents & Trademarks, Washington, D.C. 20231, on the date indicated.

Name

February 26/03
Date

#19
MJP
3/13/03

IN THE UNITED STATES PATENT AND TRADEMARK OFFICE

Inventors: Cech et al.

Filing Date: November 2, 1999

Serial No: 09/432,503

Docket: 018/063c

Title: INCREASING THE PROLIFERATIVE CAPACITY OF CELLS USING TELOMERASE REVERSE TRANSCRIPTASE

Art Unit: 1652

Examiner: Delia M. Ramirez, Ph.D.



**DECLARATION UNDER 37 CFR § 1.132**

**CALVIN B. HARLEY, Ph.D.**

Commissioner for Patents and Trademarks
Washington, D.C. 20231

Dear Sir:

I, CALVIN HARLEY, do hereby declare as follows:

1. I am the Chief Scientific Officer at Geron Corporation. I have been conducting research on telomere biology and biochemistry for over 14 years. I have 18 issued U.S. patents and over 35 academic publications on the subject.

My role at Geron is to oversee the company's entire scientific research program, including the development of human telomerase reverse transcriptase (hTRT) and telomerase inhibitors for human therapy. A copy of my curriculum vitae accompanies this Declaration.

2. I am coinventor on U.S. Patent Application referred to above. I am familiar with the contents of the application.

3. This patent application describes the isolation and characterization of the hTRT cDNA and genomic sequence, and certain functional experiments verifying its activity. The subject matter of the claims currently pending in this application is methods for increasing proliferative capacity of a mammalian cell using a nucleic acid encoding hTRT.

4. I understand the Examiner has agreed that a DNA encoding hTRT can increase the proliferative capacity of a cell *in vitro,* but questions whether this will work *in vivo*.

5. Before the making of the invention described in this disclosure and the priority applications, no one had succeeded in isolating the TRT gene from a mammalian cell. However, the biological properties of telomeres and the function of telomerase were well known (Chiu & Harley, "Replicative senescence and cell immortality: the role of telomeres and telomerase." Proc. Soc. Exp. Biol. Med. 214:99-106, 1997).

In view of this background, the makers of this invention forecast that expressing the TRT gene in a mammalian cell would cause the cell to have increased proliferative capacity. Pages 65 to 82 of the disclosure describe how hTRT can be expressed in cells. Amongst the information provided are ways of expressing hTERT encoding region under control of promoters of various kinds, nonviral expression vectors (such as plasmids and episomal vectors), and viral expression systems (such as retrovirus, adenovirus, and AAV). Pages 118 to 127 describe how expression of hTRT in cells can increase proliferative capacity. Pages 110 to 114 describe the use of telomerase expression gene therapy to increase proliferative capacity *in vivo*.

6. Shortly after discovery of the hTRT gene, the ability of hTRT to increase the proliferative capacity of cells was demonstrated *in vitro*. (Bodnar et al., "Extension of life-span by introduction of telomerase into normal human cells." Science 279:334-335, 1998. Vaziri & Benchimol, "Reconstitution of telomerase activity in normal human cells leads to elongation of telomeres and extended replicative life span." Curr. Biol. 8:279-82, 1998.). This provides direct confirmation of what was described in the patent application.

7. There is no reason to believe that hTRT would not work equally well to increase proliferative capacity *in vivo*, if delivered using an appropriate vector.

8. I understand the Examiner has already been provided with a copy of the review I wrote in 2002, entitled "Telomerase is not an Oncogene" (Oncogene 21:494-502).

There are a variety of human cell types listed in Table 1 of the article, in which TRT has been shown to cause an increase in proliferative capacity. As I explain in Figure 2, normal somatic cells transduced to express TRT may still be susceptible to the trauma or culture shock checkpoint, but if they bypass this, they will continue to proliferate beyond the replicative limit normally caused by telomere shortening.

These results show that the TRT gene by itself, delivered to isolated human cells using standard vector constructs, does act to increase proliferative capacity.

Seeing as how the effect is so wide-spread, vectors commonly used to cause expression of a recombinant gene *in vivo* would cause hTRT to be expressed in the transduced tissue in the same manner as other genes already studied. Expression of hTRT would then cause the cells to have increased proliferative capacity in the same manner as cells transduced *in vitro*.

9. Accompanying this Declaration is an article by Otto Yang, Rita Effros, and colleagues at the UCLA Medical Center in Los Angeles. It describes the effect of recombinant telomerase expression on the functional properties of cytotoxic T lymphocytes taken from AIDS patients. (J. Virol. 77:3077, 2003).

The authors of this article found that cytolytic function was impaired in CTL clones taken from patients infected with HIV-1 — attributed to clonal exhaustion of CD8(+) lymphocytes due to chronic cell turnover. The authors transduced the lymphocytes with a retroviral hTRT expression vector, provided by Geron Corporation (described in the article by Bodnar et al. referred to earlier, and constructed according to the description provided in this patent application). As a result, proliferative capacity of the CTL clones was enhanced, and cytolytic and antiviral capabilities were superior to those of control CTL.

The article concludes by proposing telomerase transduction as a therapy for immune dysfunction in chronic viral infection. Injecting the hTRT retrovirus intravenously would give the vector access to T lymphocytes in the circulation, in the same way that adding it to a culture flask allows the vector to transduce the cultured cells. The vector would have the effect of enhancing

proliferative capacity of lymphocytes *in vivo*, improving the function of the cells as described in this article.

10. Accompanying this Declaration is an article by Karl Rudolph et al. of the Dana-Faber Cancer Institute in Boston MA. It is entitled "Inhibition of Experimental Liver Cirrhosis in Mice by Telomerase Gene Delivery" (Science 287:1253-1257).

In the experiments described in the article, knockout mice were made lacking the gene for telomerase RNA component (mTR). Unlike humans, mice constitutively express TRT, but these knockout mice could not express telomerase function due to the missing mTR gene. The mice showed accelerated development of liver cirrhosis in response to a variety of insults, which correlated with the presence of shortened telomeres in these animals, due to lack of telomerase activity. Gene therapy delivering mTR back to the liver of these animals using an adenovirus vector restored telomerase activity and telomere function. The treatment alleviated cirrhotic pathology and improved liver function.

These results show that gene therapy can be used to restore telomerase function *in vivo*, having a beneficial effect attributable to increased cell survival and proliferation.

11. I understand the Examiner has already been provided with a copy of U.S. patent application 10/143,536, entitled "Treatment for Wounds", upon which I am also a named inventor.

In the experiments described in Example 6 (pages 27-30, and Figures 13-15), rabbit tissue was treated in various forms with a non-replicative adenovirus vector created by the vector biology Group at Geron Corporation. The vector contains the hTRT encoding region under control of a constitutive promoter, which causes hTRT to be expressed in transduced cells.

In the first experiment, the adenovirus hTRT vector was used to transfect cultured rabbit fibroblasts. As shown in Figure 13, the transduced fibroblasts showed does-dependent telomerase enzymatic activity, as determined by TRAP assay. In the second experiment, cultured rabbit tissue was treated in bulk with the adenovirus hTRT vector, and then subject to immunocytochemistry. As shown in Figure 14, the adenovirus vector was effective in causing hTRT expression at the protein level in the bulk tissue.

The third experiment was done *in vivo* using the established rabbit model for ischemic wounds (Ahn et al., Ann. Plast. Surg. 24:17, 1990; Wu et al., Am. J. Pathol. 154:301, 1999). The wounds were induced bilaterally by dissecting the rostral and central arteries in the ears. The wounds were then treated with $2 \times 10^9$ viral particles by local administration — either the hTRT adenovirus vector, or

vector control. Wound healing parameters were subsequently assessed in H&E stained paraffin sections. As shown in Figure 15 and Table 3, there was a dramatic increase in granulation tissue formation in the aged rabbit ear wounds treated with adenovirus hTRT, but not the control ($p < 0.01$).

Good granulation tissue is the rate-limiting impairment for robust wound closure in this ischemic wound model. Thus, seeing that the administered hTRT vector improved granulation tissue growth shows that the TRT gene can be delivered by an adenovirus vector to cells *in vivo*. These findings demonstrate the therapeutic potential of hTRT *in vivo*.

12. Accompanying this Declaration is an article by Murasawa et al. from Tufts University and the Kobi Institute, and Tokai University. It is entitled "Constitutive Human Telomerase Reverse Transcriptase Expression Enhances Regenerative Properties of Endothelial Progenitor Cells" (Circulation 106:1133-1139, 2002).

The experiments described in this publication were performed using the same hTRT adenovirus vector produced by the vector biology group at Geron Corporation. Transduction of endothelial progenitor cells (EPCs) enhanced telomerase activity, mitogenic capacity, and EGF-induced cell migration, p0romoted colony formation, and protected them from starvation-induced cell apoptosis. Genetically altered EPCs caused enhanced perfusion in a unilateral hind limb ischemia model in nude mice. Capillary density, evaluated in histological sections retrieved at day 28 from ischemic hind limb muscle, was markedly increased in mice receiving the hTRT transduced cells.

These results show that hTRT expression in cells causes increased proliferative capacity, which in turn causes enhanced tissue repair when the cells are present in ischemic tissue.

13. I hereby declare that all statements made in this Declaration of my own knowledge are true and that all statements made on information and belief are believed to be true; and further that these statements are made with the knowledge that willful false statements and the like so made are punishable by fine or imprisonment, or both, under Section 1001 of Title 18 of the United States Code, and that such willful false statements may jeopardize the validity of the application, any patent issuing thereon, or any patent to which this verified statement is directed.

2003.02.26
Date

Calvin B. Harley, Ph.D.
Menlo Park, CA

CERTIFICATE OF MAILING BY FIRST CLASS MAIL

I hereby certify that this correspondence is being deposited with the United States Postal Service as first class mail in an envelope addressed to the Commissioner for Patents & Trademarks, Washington, D.C. 20231, on the date indicated.

Name _____ Date February 26/03

IN THE UNITED STATES PATENT AND TRADEMARK OFFICE

Inventors: Cech et al.

Filing Date: November 2, 1999

Serial No: 09/432,503

Docket: 018/063c

Title: INCREASING THE PROLIFERATIVE CAPACITY OF CELLS USING TELOMERASE REVERSE TRANSCRIPTASE

Art Unit: 1652

Examiner: Delia M. Ramirez, Ph.D.

**DECLARATION UNDER 37 CFR § 1.132**

**JOHN M. IRVING, Ph.D.**

Commissioner for Patents and Trademarks
Washington, D.C. 20231

Dear Sir:

I, JOHN IRVING, do hereby declare as follows:

1. I am the Director of Molecular Biology at Geron Corporation. I have been working in the field of recombinant nucleic acid chemistry and vector construction for about 25 years. A copy of my *curriculum vitae* is enclosed with this Declaration. At Geron, I have been responsible for overseeing several different projects, such as PCR assay of gene expression in mammalian cells, and construction of viral vectors for transduction of mammalian cells, both i*n vitro* and *in vivo*.

2. I have read parts of the application referred to above that relate to construction of vectors for expressing human telomerase reverse transcriptase (hTRT). I have also read parts of patent application 10/143,536, relating to the adenovirus used in the rabbit ischemic ear model for wound healing. My group was responsible for constructing the adenovirus vector used in that study.

3. I understand the Examiner has questioned whether someone reading the application referred to above would know how to construct a vector similar to that used in the 10/143,536 application at the time that the disclosure of the present application was first filed in November 19, 1997.

4. The present application discusses various aspects of vector construction and its use in gene therapy: for example, on pages 65-82 and 110-114. Nonviral expression systems such as plasmids and episomal vectors are explained, and the reader is directed to a commercial supplier as a source of components. Viral vectors are also explained, including those based on retrovirus, adenovirus, AAV, and other systems in common use.

These systems were well known and described at the time the application was filed. See the following publications as an illustration of contemporary techniques for adenovirus and retrovirus construction:

- Graham & Prevec. Adenovirus-based expression vectors and recombinant vaccines. Biotechnology 290:363, 1992.
- Sime, Xing, Foley, Graham & Gauldie. Transient gene transfer and expression in the lung. Chest 111:89S, 1997.
- He, Zhou, da Costa, Yu, Kinzler & Vogelstein. A simplified system for generating recombinant adenoviruses. Proc. Natl. Acad. Sci. USA 95:25009, 1998.
- Anton & Graham. Site-specific recombination mediated by an adenovirus vector expressing the Cre recombinase protein: a molecular switch for control of gene expression. J. Virol. 69:4600, 1995.
- Hitt, Addison & Graham. Human adenovirus vectors for gene transfer into mammalian cells. Adv. Pharmacol. 40:137, 1997.
- Graham et al. Adenovirus vectors for gene therapy. PCT publications WO 95/00655 and WO 96/40955 (now U.S. patents 5,919,676; 6,120,764; and 6.140,087, assigned to Advec, Inc).

- Pear, Nolan, Scott & Baltimore. Production of high-titer helper-free retroviruses by transient transfection. Proc. Natl. Acad. Sci. USA 90:8392, 1993.
- Kinsella & Nolan. Episomal vectors rapidly and stably produce high-titer recombinant retrovirus. Hum Gene Ther 7:1405, 1996.
- Lindemann, Patriquin, Feng & Mulligan. Versatile retrovirus vector systems for regulated gene expression *in vitro* and *in vivo*. Mol Med 3:466, 1997.
- Sadelain, Wang, Antoniou, Grosveld & Mulligan. Generation of a high-titer retroviral vector capable of expressing high levels of the human β-globin gene. Proc. Natl. Acad. Sci. USA 92:6728, 1995.

5. If I wanted to make an hTRT expression vector in 1997, based on the discussion in the disclosure, I would have proceeded according to the same principles of vector construction that would be employed by any reader with appropriate experience.

A typical procedure might be as follows: two plasmids would be prepared by recombinant DNA techniques using bacterial cells. One would contain the adenovirus backbone, missing the left-hand ITR and the E1 region, but including the rest of the adenovirus encoding region up to the right-hand ITR. The other would be a small shuttle plasmid. It would contain the left-hand ITR and packaging signals, followed by an expression cassette containing the hTRT encoding region under control of a suitable promoter replacing the E1 region. The expression cassette is flanked by two regions of 2 kb or more of adenovirus sequence shared with the backbone plasmid, permitting homologous recombination. The hTRT encoding sequence is provided in the disclosure, and could be cloned from any suitable library as described. A number of promoters would work. Many of the promoters listed on page 67 of the specification would be good choices.

The two plasmids would then be opened with a restriction nuclease, and co-transfected into a eukaryotic host cell that could supply E1 function in trans. 293 cells are typically used for this purpose. Suitable transfection protocols known at the time were the calcium-phosphate method, and the lipofection method. The plasmids would assemble together in the host cell by homologous recombination, replicate in the cytoplasm, and be packaged into replication-incompetent adenovirus vectors.

6. In the 10/143,536 application, an hTRT adenovirus vector is described in Example 4, and then used in the ischemic ear model in Example 6. This adenovirus vector was constructed by the vector group at Geron Corporation under my supervision. We used the commercially available AdMax™ system obtained from Microbix Biosystems Inc., Toronto Canada, which distributes kits on behalf of Advec, Inc. This system again uses an adenovirus backbone plasmid and a shuttle plasmid. Recombination is effected not by homologous regions in the plasmid, but by site-specific recombination using the Flp/*frt* system which is somewhat more efficient.

Use of site-specific recombinase enzymes for assembling adenoviruses were already known and in use (WO 96/40955) at the time the present disclosure was first filed. Transcription is driven in our hTRT vector by the CAG system, containing the CMV enhancer and a modified chicken beta-actin promoter. The CAG system was also known (Kiwake, Endo et al., Hum Gene Ther 7:821, 1996) at the time this disclosure was first filed.

7. The adenovirus vector made using the AdMax™ system for the 10/143,536 application contains an hTRT expression cassette in essentially the same functional arrangement as the vector made by homologous recombination in the manner described above. A vector made by homologous recombination would be expected to perform in the experiments described in the 10/143,536 application in a similar fashion.

8. I hereby declare that all statements made in this Declaration of my own knowledge are true and that all statements made on information and belief are believed to be true; and further that these statements are made with the knowledge that willful false statements and the like so made are punishable by fine or imprisonment, or both, under Section 1001 of Title 18 of the United States Code, and that such willful false statements may jeopardize the validity of the application, any patent issuing thereon, or any patent to which this verified statement is directed.

1-31-03
Date

John M. Irving
John M. Irving, Ph.D.
Menlo Park, CA

the γ-ray emission. The $K_{\alpha,\beta}$ x-rays originate from the subsequent filling of the holes in the K shell.
17. The Fe foil had a purity of 99.95% and was enriched to 95% in the $^{57}$Fe isotope. Because the atomic mass of the probe atom is 57u and that of the lattice atoms is close to 57u (where u is the atomic mass unit), all results exhibit a systematic deviation from natural Fe (55.86u) in the range of 1 to 2%. This deviation is smaller than the present experimental uncertainty, however it should be considered in all studies with $^{57}$Fe.
18. A. Jayaraman, *Rev. Mod. Phys.* **55**, 65 (1983).
19. V. J. Minkiewicz, G. Shirane, R. Nathans, *Phys. Rev.* **162**, 528 (1967). The DOS is tabulated by H. R. Schober and P. H. Dederichs, in *Landolt-Börnstein*, K.-H. Hellwege and J. L. Olsen, Eds. (Springer-Verlag, Berlin, 1981), vol. III/13a, pp. 53–56.
20. K. S. Singwi and A. Sjölander, *Phys. Rev.* **120**, 1093 (1960).
21. J. D. Althoff, P. B. Allen, R. M. Wentzcovitch, J. A. Moriarty, *Phys. Rev. B* **48**, 13253 (1993).
22. Debye temperatures can be calculated alternatively from the Lamb-Mössbauer factor, the low-temperature specific heat, or the low-energy part of the phonon DOS, thus providing slightly different data sets reflecting mainly deviations of the lattice dynamics from a perfect Debye-like behavior.
23. W. Jones and N. H. Marsh, *Theoretical Solid State Physics* (Dover, New York, 1985), vol. 1, p. 237.
24. V. G. Kohn, A. I. Chumakov, R. Rüffer, *Phys. Rev. B* **58**, 8437 (1998).
25. H. K. Mao, Y. Wu, L. C. Chen, J. F. Chu, A. P. Jephcoat, *J. Geophys. Res.* **95**, 21737 (1990).
26. J. Ramakrishnan, R. Boehler, G. H. Higgins, G. C. Kennedy, *J. Geophys. Res.* **83**, 3535 (1978).
27. G. Simmons and H. Wang, *Single Crystal Elastic Constants and Calculated Aggregate Properties* (MIT Press, Cambridge, MA, 1971). The described procedure of calculating $v_p$ and $v_s$ from elastic constants was used also for results from (*29*, *30*).
28. L. Stixrude and R. E. Cohen, *Science* **267**, 1972 (1995); see also (*31*).
29. P. Söderlind, J. A. Moriarty, J. M. Wills, *Phys. Rev. B* **53**, 14063 (1996).
30. A. Singh, H.-K. Mao, J. Shu, R. J. Hemley, *Phys. Rev. Lett.* **80**, 2157 (1998).
31. H.-K. Mao *et al.*, *Nature* **396**, 741 (1998); *Nature* **399**, 280 (1999).
32. D. Alfè, M. J. Gillan, G. D. Price, *Nature* **401**, 462 (1999).
33. A. Snigirev *et al.*, *Nature* **384**, 49 (1996).
34. A. K. Freund *et al.*, *Proc. SPIE* **3448**, 1 (1998).
35. We thank the Microfluorescence group (ID22) and the Nuclear Resonance group (ID18) of the ESRF for preparation of nuclear resonance station ID22N and for their help during the experiment, A. Snigirev and A. K. Freund for their expert help with the focusing elements, and K. Rupprecht and H. Giefers for their assistance with the measurements. We acknowledge useful discussions with W. B. Holzapfel, R. Rüffer, G. Shen, and W. Sturhahn. Supported by the Bundesministerium für Bildung, Wissenschaft, Forschung und Technologie (project 05 SK8PPA).

11 November 1999; accepted 29 December 1999

# Inhibition of Experimental Liver Cirrhosis in Mice by Telomerase Gene Delivery

**Karl Lenhard Rudolph,[1] Sandy Chang,[1,2] Melissa Millard,[1] Nicole Schreiber-Agus,[3] Ronald A. DePinho[1]***

**Accelerated telomere loss has been proposed to be a factor leading to end-stage organ failure in chronic diseases of high cellular turnover such as liver cirrhosis. To test this hypothesis directly, telomerase-deficient mice, null for the essential telomerase RNA (mTR) gene, were subjected to genetic, surgical, and chemical ablation of the liver. Telomere dysfunction was associated with defects in liver regeneration and accelerated the development of liver cirrhosis in response to chronic liver injury. Adenoviral delivery of mTR into the livers of mTR$^{-/-}$ mice with short dysfunctional telomeres restored telomerase activity and telomere function, alleviated cirrhotic pathology, and improved liver function. These studies indicate that telomere dysfunction contributes to chronic diseases of continual cellular loss-replacement and encourage the evaluation of "telomerase therapy" for such diseases.**

Cirrhosis of the liver is the seventh leading cause of death by disease, affecting several hundred million people worldwide (*1*). In this chronic disease, a diverse array of hepatotoxins, ranging from chronic viral hepatitis to alcohol, promotes continual hepatocyte destruction that, in turn, stimulates abnormal patterns of hepatocyte regeneration and fibrous scarring over many years (*2*). The resulting distortion of the liver architecture compromises hepatocyte function, causing systemic life-threatening complications. Left unchecked, this pathological process culminates in fatal end-stage liver failure, marked by extensive fibrotic replacement and cessation of hepatocyte proliferation (*2*, *3*).

Liver cirrhosis is characterized by the conversion of hepatic stellate cells into activated, myofibroblast like cells (*2*). It has been postulated that hepatocyte destruction itself serves as an activation signal for this conversion, possibly by the release of insulin-like growth factor or lipid peroxides from apoptotic cells (*2*). Therefore, factors that govern the survival of hepatocytes could potentially influence stellate cell activation and fibrogenesis.

The second key aspect of terminal liver failure, hepatocyte proliferative arrest, has been linked to several etiologic factors including altered hepatocyte-matrix interactions (*2*), growth inhibition by abundant transforming growth factor–β1 (TGF-β1) (*4*), and/or critical telomere shortening. The telomere hypothesis is a particularly appealing one, because sustained hepatocyte turnover accelerates the pace of telomere attrition in the human cirrhotic liver (*5*), thereby presumably activating senescence or crisis checkpoints. The importance of telomere maintenance in long-term cellular and organ homeostasis has been experimentally verified in cultured human cells and in telomerase-deficient mice (*6*, *7*). These mice lack the telomerase RNA (mTR) gene and show progressive telomere shortening from one generation to the next. In late-generation mice (e.g. generation 6), telomere dysfunction and genomic instability are associated with impaired proliferation and/or apoptosis in organ systems with high renewal requirements, such as the bone marrow and the gut (*8*). In contrast, the liver is unperturbed and appears to function and develop normally even in late-generation mTR$^{-/-}$ mice (*9*). Here we use the mTR$^{-/-}$ mice to evaluate the role of telomere shortening in chronic liver disease. Liver injury was induced in these animals by three experimental procedures to gauge how telomere shortening influences hepatocyte proliferation, survival, and ultimately predisposition to cirrhosis.

The first system, the albumin-directed urokinase plasminogen activator (Alb-uPA) transgenic mouse, allows investigation of the factors governing hepatocyte regenerative capacity. Alb-uPA expression has been shown to cause widespread hepatocyte death and liver failure in newborn mice (*10*). However, 60% of hemizygous transgenic mice survive as a result of spontaneous transgene deletion in rare hepatocytes that then clonally expand to reconstitute the entire organ by 3 months of age (*11*). To assess the impact of loss of telomerase activity and telomere shortening on liver regeneration capacity, we monitored Alb-uPA transgene transmission as well as phenotypic differences in mTR$^{+/+}$ mice and successive generations of mTR$^{-/-}$ mice (*12*). Consistent with previous reports (*11*), we observed transmission rates of 31% for mTR$^{+/+}$ and 27% for second-generation (G2) mTR$^{-/-}$ mice (Fig. 1A). Because the

[1]Department of Adult Oncology, Medicine and Genetics, Dana-Farber Cancer Institute, 44 Binney Street (M413), and Harvard Medical School, Boston, MA 02115, USA. [2]Department of Pathology, Brigham and Women's Hospital and Harvard Medical School, Boston, MA 02115, USA. [3]Department of Molecular Genetics, Albert Einstein College of Medicine, Bronx, NY 10461, USA.

*To whom correspondence should be addressed. E-mail: ron_depinho@dfci.harvard.edu

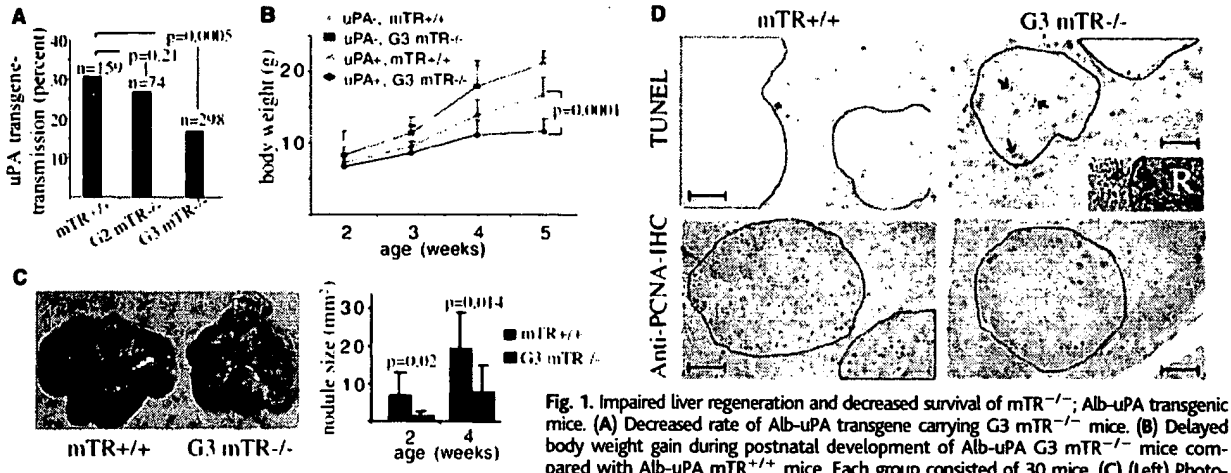


Fig. 1. Impaired liver regeneration and decreased survival of mTR$^{-/-}$; Alb-uPA transgenic mice. (A) Decreased rate of Alb-uPA transgene carrying G3 mTR$^{-/-}$ mice. (B) Delayed body weight gain during postnatal development of Alb-uPA G3 mTR$^{-/-}$ mice compared with Alb-uPA mTR$^{+/+}$ mice. Each group consisted of 30 mice. (C) (Left) Photograph of whole livers of 4-week-old Alb-uPA mTR$^{+/+}$ mice and Alb-uPA G3 mTR$^{-/-}$ mice. Smaller regenerative nodules (red) in Alb-uPA G3 mTR$^{-/-}$ liver are apparent. (Right) Histogram representation of nodule size in 2- and 4-week-old mice. Each group had 16 to 20 mice. (D) Photomicrographs of TUNEL (top) and PCNA immunohistochemistry (bottom) of liver sections from Abl-uPA mTR$^{+/+}$ and Alb-uPA G3 mTR$^{-/-}$ mice. Increased numbers of TUNEL-positive cells (arrows) can be seen in the regenerative nodule (circled) in mTR$^{-/-}$ mice (bar: 100 μm). (Inset) H&E stain of the border of a regenerative nodule (R, right) and the transgene-expressing liver (left) (bar: 100 μm). PCNA immunostaining (bottom) of regenerating livers demonstrated decreased staining within regenerative nodules (circled) of 5-week-old Alb-uPA G3 mTR$^{-/-}$ mice compared with age-matched Alb-uPA mTR$^{+/+}$ mice (bar: 100 μm).

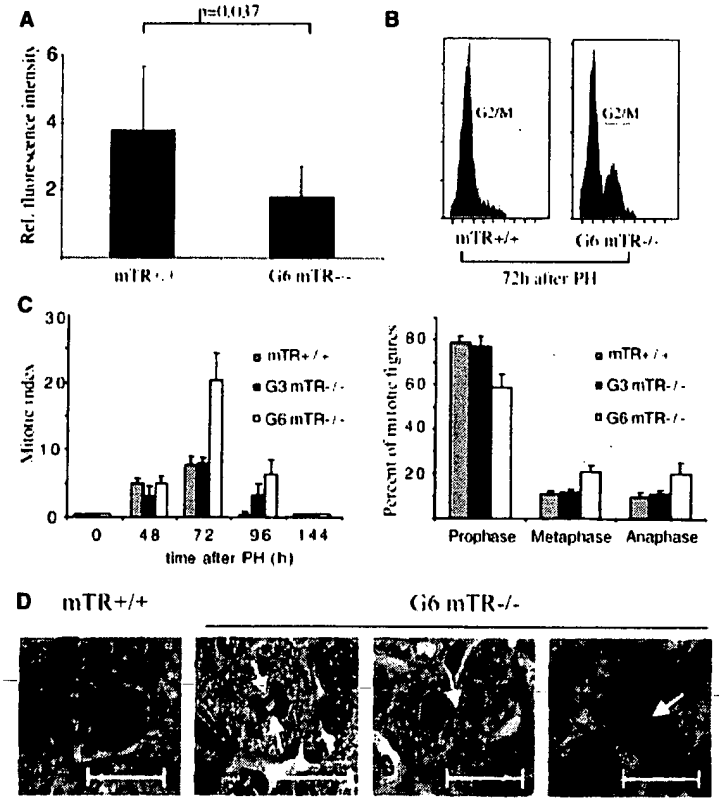


Fig. 2. Impaired cell cycle progression and anaphase bridging in regenerating mTR$^{-/-}$ livers after partial hepatectomy. (A) Telomere length of peripheral blood lymphocytes determined by Flow-FISH (*13*) in 8 mTR$^{+/+}$ and 10 G6 mTR$^{-/-}$ mice before PH. (B) G2/M cell cycle block in regenerating hepatocytes of G6 TR$^{-/-}$ mice 72 hours after PH, as determined by flow cytometry. (C) Delayed progression through mitosis results in an increase in the mitotic index (left) and a shift from prophase to anaphase and metaphase (right) in regenerating livers of G6 mTR$^{-/-}$ mice compared with livers from mTR$^{+/+}$ mice or G3 mTR$^{-/-}$ mice (eight mice per group). (D) Anaphase bridges in H&E-stained regenerating liver sections of G6 mTR$^{-/-}$ mice 48 to 96 hours after PH. The arrows point to chromatin bridges between the separating chromosomes. Anaphase from a mTR$^{+/+}$ control liver is shown on the left for comparison (bars: 20 μm).

G2 mTR$^{-/-}$ mice are telomerase-deficient yet still possess long, intact telomeres (*7*), it appears that telomerase activity itself is not a key determinant of hepatocyte regeneration potential. In contrast, a decrease in transgene transmission (16% transgene-positive on postnatal day 12) and reciprocal rise in perinatal deaths became evident in G3 mTR$^{-/-}$ mice (Fig. 1A). In addition, the few surviving Alb-uPA G3 mTR$^{-/-}$ mice exhibited reduced fitness and poor weight gain relative to Alb-uPA mTR$^{+/+}$ controls, whereas nontransgenic G3 mTR$^{-/-}$ and mTR$^{+/+}$ animals were phenotypically indistinguishable (Fig. 1B). Flow–fluorescence in situ hybridization (FISH) telomere length measurements of peripheral blood lymphocytes documented the expected progressive decline in telomere lengths from G1 to G3 (*7, 13*).

To assess clonal liver regeneration potential in the surviving Alb-uPA transgenic mice, we monitored the growth of regenerative liver nodules, which are estimated to arise from about 20 cell doublings of a single transgene-negative hepatocyte (*11*). Impaired growth of regenerative nodules in the Alb-uPA G3 mTR$^{-/-}$ livers was first detectable by 2 weeks of age and most pronounced by week 4 (Fig. 1C). The impaired macroscopic growth of regenerative nodules in mice with shorter telomeres correlated with a 3.6-fold increase in TUNEL (terminal deoxynucleotidyl transferase dUTP nick-end labeling)–positive apoptotic cells in the regenerative nodules (Fig. 1D, top) ($P = 0.003$) and a decrease in proliferating cell nuclear antigen (PCNA)–positive S phase cells (Fig. 1D, bottom).

The second approach we used to test liver regenerative capacity was partial hepatectomy (PH), surgical removal of two-thirds of


Fig. 6. Reactiv
mice. (A) Mas
treatment sho
mTR$^{-/-}$ mice
(bar: 200 μm).
Ad-GFP–treate
apparent in Ac
showed decrea
Ad-GFP–treate

liver regenera
aphase bridges
double-strand
DNA damage
arrest and inc
lipid peroxide
cytes) and/or
tors such as T
cell activation
telomere short
cells to cope
minished oxid
resulting in in
cal of end-stag

Our study i
ing contribute
cirrhosis and t
beneficial for
these animal-b
significant red
in human cirr
range associat
senescence an
ity (*28*). In th
associated mo
replicative sen
responses conv
ical end points

the liver (*14*). In this procedure greater than 50% of hepatocytes follow a highly synchronized cell cycle reentry pattern, reaching peak S-phase activity at 24 to 48 hours, maximal mitosis at 72 hours, and cessation of cell division at 96 hours after PH. After this regenerative wave, normal organ histology is reestablished within 1 week (*15*). Consistent with the shorter telomere length of G6 mTR$^{-/-}$ mice (Fig. 2A), the liver mass of G6 mTR$^{-/-}$ mice at 72 hours after PH was reduced relative to mTR$^{+/+}$ controls, despite comparable liver weight in G6 mTR$^{-/-}$ and mTR$^{+/+}$ mice not subjected to PH (*9*). In addition, although all mTR$^{+/+}$ mice were found to be free of lethal postoperative complications, 3 of the 10 G6 mTR$^{-/-}$ mice died 48 to 72 hours after PH. Interestingly, these compromised mice had shorter telomeres than the G6 mTR$^{-/-}$ survivors (*9*).

The impaired regeneration of post-PH livers of surviving G6 mTR$^{-/-}$ mice prompted us to analyze the regenerative profile of G6 mTR$^{-/-}$ hepatocytes by flow cytometry, mitotic index determination, and bromodeoxyuridine labeling. These cells showed a normal onset of S phase at 24 hours after PH (*9*). In contrast, at 72 hours after PH, flow cytometry of cells from the regenerating liver front (*16*) revealed a two- to threefold increase in the $G_2$/M fraction of G6 mTR$^{-/-}$ hepatocytes relative to mTR$^{+/+}$ and G3 mTR$^{-/-}$ controls (Fig. 2B). This effect was also apparent microscopically as an increase in the number of mitotic figures (Fig. 2C). Further classification of the mitotic profile demonstrated a decrease in the prophase fraction and a compensatory increase in the metaphase/anaphase fraction (Fig. 2C). These data are consistent with impaired cell progression through mitosis, as opposed to a higher number of cells entering mitosis. We propose that telomere loss may interfere with progression through mitosis because of the production of end-to-end chromosomal fusions, opposing kinetochore alignment, and anaphase bridges (*17*). Indeed, hemotoxylin and eosin (H&E)–stained liver sections at 48 to 96 hours after PH showed many aberrant mitotic figures and anaphase bridges only in the G6 mTR$^{-/-}$ liver samples (Fig. 2D). Together, these findings indicate that telomere dysfunction delays the mitotic progression of regenerating G6 mTR$^{-/-}$ hepatocytes and in turn delays the restoration of liver mass after surgical hepatectomy.

The third approach we used to assess the impact of telomere dysfunction on liver regeneration was repeated toxin-mediated liver injury, which is known to culminate in liver cirrhosis. In humans, cirrhosis often results from the accumulated effects of years of sustained hepatocyte destruction and subsequent regeneration. This can be modeled in mice by repeated exposure to hepatotoxins such as $CCl_4$ (*18*). In mice, 12 to 18 repeated applications of $CCl_4$ are required to induce modest liver cirrhosis, which is thought to be mechanistically linked to hepatocyte necrosis (*18*). Given the long length of mouse telomeres (*19*), the promiscuous somatic expression of telomerase in the mouse liver, and the limited number of cell divisions after $CCl_4$ treatment, the mTR$^{-/-}$ mouse affords a system in which to test whether telomere dysfunction limits hepatocyte function and accelerates the development of liver cirrhosis.

One consistent feature of the cirrhotic patient is poor weight gain due to several factors including hypermetabolism, malabsorption, recurrent infections, and poor appetite (*20*). Another feature of the cirrhotic condition is impaired bile drainage (cholestasis), leading to persistently elevated serum bilirubin levels and jaundice (*21*). After 3 months of $CCl_4$ treatment (*22*), the G6 mTR$^{-/-}$ mice showed significantly impaired gain of body weight compared with mTR$^{+/+}$ or G3 mTR$^{-/-}$ mice. After 6 months of $CCl_4$ administration, poor weight gain persisted in G6 mTR$^{-/-}$ mice and became manifest in G3 mTR$^{-/-}$ mice as well (Fig. 3A). Marked increases of serum bilirubin levels were also seen in the G6 mTR$^{-/-}$ mice after only two rounds of $CCl_4$ (Fig. 3B). Finally, liver sections of mTR$^{+/+}$ and G3 mTR$^{-/-}$ mice, treated v six rounds of $CCl_4$, exhibited mild lipid ac mulation (steatosis) and minimal fibrosis (I 3C), whereas comparable sections from mTR$^{-/-}$ mice showed pronounced steato centrilobular fibrosis, and inflammatory l phocytic infiltrates—hallmarks of chronic patic injury and cirrhosis (Fig. 3C).

To determine if telomerase administrat could block the development of cirrhosis mice with dysfunctional telomeres, we c structed adenoviral vectors that would dir the expression of GFP (green fluorescent p tein) alone or mTR-GFP to the livers mTR$^{+/+}$ and G6 mTR$^{-/-}$ mice (*23*). In th studies, we verified that the mean telom length in lymphocytes of G6 mTR$^{-/-}$ m was ~70% reduced compared with that mTR$^{+/+}$ mice (Fig. 4A). Forty-eight ho after delivery of $1 \times 10^{12}$ viral particles tail vein injections, telomerase activity detected in the liver but not in the spleen G6 mTR$^{-/-}$ mice infected with the Ad-m GFP virus (Fig. 4B, compare lane 5 with l 4), consistent with the strong liver tropism adenovirus (*24*). Liver cryosections obtai at the same time demonstrated GFP fluo cence in 85 to 100% of liver cells.

We next examined whether cirrh could be inhibited in G6 mTR$^{-/-}$ mice

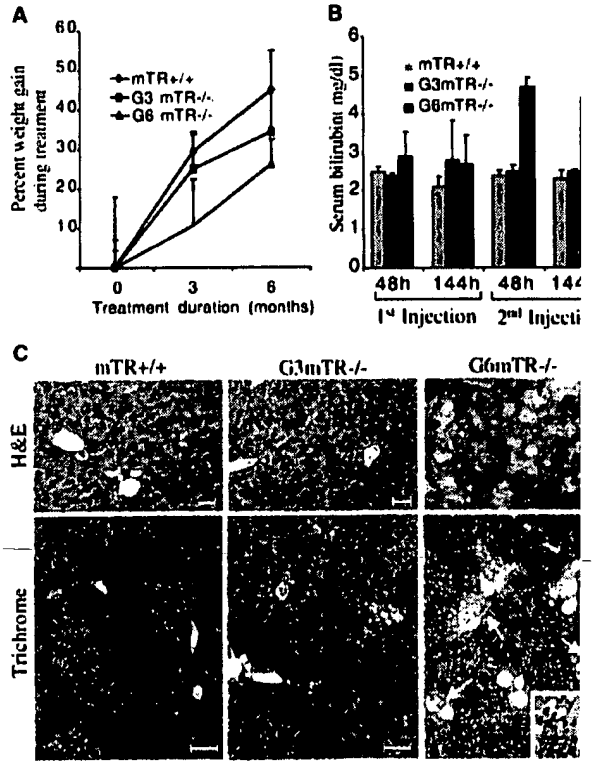


Fig. 3. Telomere shortening accelerates the development of cirrhosis in response to chronic liver damage. (A) Reduced body-weight gain in G6 mTR$^{-/-}$ mice compared with G3 mTR$^{-/-}$ and mTR$^{+/+}$ mice after repeated liver injury (monthly injections of 10 μl of 10% $CCl_4$ per gram of body weight), with six mice examined per group. (B) A twofold increase of serum bilirubin in G6 mTR$^{-/-}$ mice compared with similarly treated G3 mTR$^{-/-}$ and mTR$^{+/+}$ mice (six mice per group) was seen after the second injection of $CCl_4$. (C) H&E-stained (upper; bar: 50 μm) and Masson-trichrome–stained (lower; bar: 100 μm) liver sections of mTR$^{+/+}$, G3 mTR$^{-/-}$, and G6 mTR$^{-/-}$ mice 6 months after repeated $CCl_4$-induced liver injury. Marked steatosis (vacuolated appearance) and fibrosis (blue stain with Massan-trichrome, arrows) are evident in livers of G6 mTR$^{-/-}$ mice but not in livers of mTR$^{+/+}$ and G3 mTR$^{-/-}$ mice. (h High-power view of collagen deposition (blue stain) in the centrilobular areas of G6 mTR$^{-/-}$ mice (ba μm).

JOURNAL OF VIROLOGY, Mar. 2003, p. 3077–3083 Vol. 77, No. 5
0022-538X/03/$08.00+0 DOI: 10.1128/JVI.77.5.3077–3083.2003


# Differential Impairment of Lytic and Cytokine Functions in Senescent Human Immunodeficiency Virus Type 1-Specific Cytotoxic T Lymphocytes

Mirabelle Dagarag,[1] Hwee Ng,[2] Rachel Lubong,[2] Rita B. Effros,[1] and Otto O. Yang[2]*

*Departments of Pathology and Laboratory Medicine[1] and Medicine (Division of Infectious Diseases),[2] Geffen School of Medicine, UCLA Medical Center, Los Angeles, California*

Received 29 October 2002/Accepted 4 December 2002

**Telomere length is abnormally short in the CD8$^+$ T-cell compartment of human immunodeficiency virus type 1 (HIV-1)-infected persons, likely because of chronic cell turnover. Although clonal exhaustion of CD8$^+$ cytotoxic T lymphocytes (CTL) has been proposed as a mechanism for loss of antigen-specific responses, the functional consequences of exhaustion are poorly understood. Here we used telomerase transduction to evaluate the impact of senescence on CTL effector functions. Constitutive expression of telomerase in an HIV-1-specific CTL clone results in enhanced proliferative capacity, in agreement with prior studies of other human cell types. Whereas the CTL remain phenotypically normal in terms of antigenic specificity and requirements for proliferation, their cytolytic and antiviral capabilities are superior to those of control CTL. In contrast, their ability to produce gamma interferon and RANTES is essentially unchanged. The selective enhancement of cytolytic function in memory CTL by ectopic telomerase expression implies that loss of this function (but not cytokine production) is a specific consequence of replicative senescence. These data suggest a unifying mechanism for the in vivo observations that telomere lengths are shortened in the CD8$^+$ cells of HIV-1-infected persons and that HIV-1-specific CTL are deficient in perforin. Telomerase transduction could therefore be a tool with which to explore a potential therapeutic approach to an important pathophysiologic process of immune dysfunction in chronic viral infection.**

Human T lymphocytes have the capacity to undergo a finite number of cell divisions before entering replicative senescence, a state in which cells remain metabolically active but are incapable of further proliferation (14). A major feature of replicative senescence is the erosion of telomeres, the hexameric sequences located at the distal ends of eukaryotic chromosomes, which function to stabilize the chromosome and progressively shorten in length with each cell division (1, 5, 15). Telomeres and their accessory binding proteins are thought to serve as a mitotic counter of the number of divisions a cell has completed, triggering cell cycle arrest and replicative senescence when the telomere length is too short to ensure chromosomal integrity (7, 31). Cell senescence is thus considered to be a protective mechanism that prevents unlimited growth and tumorigenesis (12).

T-cell clonal exhaustion in individuals chronically infected with human immunodeficiency virus type 1 (HIV-1) has been proposed as a mechanism of immune failure (3, 14). In support of this notion, abnormally short telomere length in the CD8$^+$ T-cell compartment of infected individuals has been documented (13, 27, 36), suggesting that infection induces excessive CD8$^+$ T-cell turnover and/or activation, leading to accelerated telomere shortening and premature senescence. This observation has significant implications, because CD8$^+$ cytotoxic T lymphocytes (CTL) are believed to play a pivotal protective role in HIV-1 infection (42). CTL are thought to suppress viremia in acute infection (8, 21) and chronic infection (26) and are potent inhibitors of HIV-1 replication in vitro (11, 40), yet it is unknown why they ultimately fail to control infection in the majority of infected persons (22). During the asymptomatic phase of infection, viral replication in vivo has been estimated at approximately $10^{10}$ virions per day (17, 34), and thus, CTL face a continuous antigenic challenge over years of infection. Replicative senescence due to chronic turnover and exhaustion is therefore a potential contributing factor in the eventual failure of cellular immunity in HIV-1 infection (13).

Recent studies have demonstrated that transfection and constitutive expression of the catalytic subunit of human telomerase reverse transcriptase (hTERT) in various primary human cell types results in telomere lengthening and an increased proliferative life span with no apparent phenotype alteration (7, 31, 38). This strategy may therefore be useful in preventing replicative senescence in cells undergoing chronic turnover. Two published studies have examined the effects of constitutive telomerase expression on CD8$^+$ T lymphocytes. Rufer et al. (28) demonstrated that hTERT transduction of naive CD8$^+$ T-cell clones extends their ability to proliferate over time without detectable alteration of phenotype or function, and Hooijberg et al. (18) achieved similar results with a melanoma-specific CD8$^+$ memory T-cell clone. However, it is unclear what effect telomerase has on virus-specific memory effector T cells that have proliferated to near senescence in response to antigen from a pathogen. In the case of HIV-1, persistent exposure to antigen leads to continuous turnover of virus-specific CTL over years. In this study, we evaluated the effects of telomerase transduction on HIV-1-specific CTL and

* Corresponding author. Mailing address: Division of Infectious Diseases, 37-121 Center for Health Sciences, 10833 LeConte Ave., UCLA Medical Center, Los Angeles, CA 90095-1688. Phone: (310) 794-9491. Fax: (310) 825-3632. E-mail: oyang@mednet.ucla.edu.

addressed the potential functional impact of telomerase on memory T cells near the end of their replicative life span.

## MATERIALS AND METHODS

**Polyclonal CD8$^+$ T-cell lines.** CD8$^+$ cell lines were derived from the peripheral blood mononuclear cells (PBMC) of HLA A*0201 HIV-1-seropositive participants in the Los Angeles Multicenter AIDS Cohort Study. These CTL-enriched lines were produced by coculturing $4 \times 10^6$ freshly Ficoll-isolated PBMC with $10^6$ autologous peptide-pulsed PBMC (previously labeled with synthetic peptide SLYNTVATL, ILKEPVHGV, or LWVTVYYGV at 10 μg/ml for 90 min) in Yssel's T-cell medium (Gemini Bio-Products, Woodland, Calif.) supplemented with L-glutamine, penicillin and streptomycin (both from Cellgro, Herndon, Va.), and recombinant interleukin-2 (IL-2; Roche Diagnostics, Indianapolis, Ind.). After 10 to 14 days, the CD8$^+$ T cells were purified by magnetic cell sorting (Miltenyi Biotec, Auburn, Calif.) and plated at $4 \times 10^6$ cells/well of a 12-well plate in Yssel's T-cell medium supplemented with 150 IU of IL-2 per ml. Cells were transduced with hTERT or the vector control at 4 weeks after primary stimulation and restimulated every 3 to 4 weeks with irradiated autologous peptide-pulsed Epstein-Barr virus-transformed B cells. Population doublings were determined by counting viable cells every 1 to 2 weeks.

**HIV-1-specific CTL.** HIV-1 specific CTL clone 68A62 was obtained from the blood of an infected individual by cloning of PBMC at limiting dilution and characterized for specificity and HLA restriction as previously described (33). This clone recognized the A2-restricted epitope ILKEPVHGV (IV9) in reverse transcriptase (amino acids 309 to 317 in HXB2) and was carried in long-term culture by weekly restimulation with anti-CD3 antibody and irradiated allogeneic feeder PBMC with IL-2 as previously described (33). Each restimulation was performed on $10^6$ CTL in a total volume of approximately 15 ml. Concentrations of viable cells were determined manually by light microscopy of trypan blue-exposed cells after each weekly expansion.

**Amphotropic viral transduction vector containing hTERT.** The amphotropic PA317 packaging cell line (derived from the ecotropic packaging cell line PE501) containing stably transfected retroviral vector pBABE with hTERT cDNA (cloned from pGRN145) (7) was provided by Geron Corporation (Menlo Park, Calif.). Supernatants containing retrovirus were harvested from plates at 40 to 60% confluence, passed through a 0.45-μm-pore-size filter, and used to infect CTL.

**Transduction of CD8$^+$ T cells and CTL with hTERT.** Two days after restimulation, the cells were cultured on RetroNectin (Takara Shuzo Co., Shiga, Japan)-precoated T25 flasks (Falcon) and transduced with hTERT vector, empty control vector, or no vector for 18 h. After transduction, the CTL were passaged in parallel with weekly restimulations. Clone 68A62 was successfully transduced twice in independent experiments.

**Calculation of cell doublings.** After restimulations of polyclonal CD8$^+$ T cells and CTL clones, the increase in the number of cells was used to estimate cell doublings in accordance with the following formula: doublings = $\log_2$(final cell concentration/initial cell concentration). The sum of all prior doublings in previous restimulations was designated the cumulative doublings of a cell line.

**Measurement of telomerase activity (TRAP assay).** A modified telomeric repeat amplification protocol (TRAP) assay was used to detect telomerase activity (20). Measurement of telomerase activity in transduced and control CTL was performed with lysates of $10^4$ cells by using the TRAPeze kit (Oncor, Gaithersburg, Md.) in accordance with the manufacturer's protocol. The resulting PCR products were then electrophoresed on a 10% 19:1 acrylamide/bisacrylamide gel, followed by Phosphorimager analysis (Packard, Downers Grove, Ill.) to visualize and quantitate the products.

**Chromium release assays.** Standard chromium release assays were performed by using transduced and control CTL as effector cells (39). In brief, T1 cells (expressing HLA A2) were labeled with 50 μCi of $^{51}$Cr in the presence or absence of the IV9 peptide at 10 μg/ml for 1 h. These cells were then washed and plated in a 96-well U-bottom plate at $10^4$ cells/well. CTL were then added at the indicated ratios for a 4-h incubation, after which supernatant was analyzed by scintillation counting for $^{51}$Cr (MicroBeta 1450; EG&G Wallac). Spontaneous release was determined in the absence of CTL, and maximal release was determined in the presence of 2.5% Triton X-100 (Sigma). All wells were run in duplicate or triplicate, and specific lysis was calculated as follows: (experimental release − spontaneous release)/(maximal release − spontaneous release).

**Peptide-major histocompatibility complex (MHC) tetramer analysis.** Allophycocyanin-labeled HLA A2 tetramer containing the ILKEPVHGV peptide was obtained from the National Institute of Allergy and Infectious Diseases MHC Tetramer Core Facility. Staining was performed by incubating CTL with a pretitrated dilution of tetramer for 30 min at 4°C as previously described (26). Cells were then analyzed by using a FACScalibur flow cytometer and CellQuest software (Becton Dickinson).

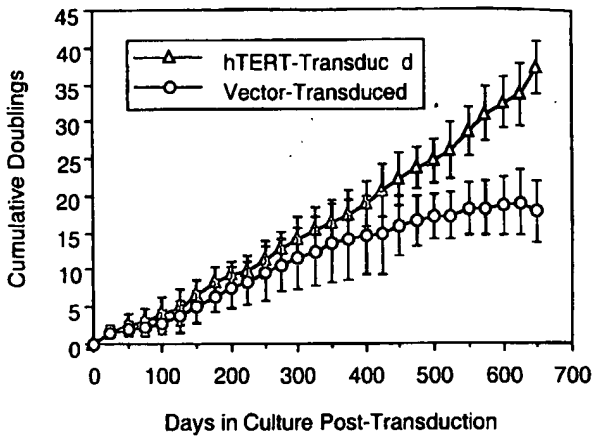


FIG. 1. Proliferation of hTERT-transduced polyclonal CD8$^+$ cells from HIV-1-infected individuals. Low-passage peptide-stimulated CD8$^+$ T-cell lines derived from the PBMC of five persons were transduced with hTERT or the control vector. The cells were restimulated approximately every 3 weeks. Mean cumulative cell doublings (the number of twofold increases required to achieve the change in cell numbers after restimulations) over time are plotted for transduced versus nontransduced lines. Error bars represent 1 standard deviation.

**Intracellular cytokine measurement.** Standard intracellular cytokine staining for gamma interferon (IFN-γ) or RANTES was performed by using commercial reagents (BDBiosciences, San Diego, Calif.). Briefly, cells were first stimulated for 6 h with the anti-CD3 antibody 12F6 (37) at 1 μg/ml in the presence of 1 μg of monensin per ml. The cells were then surface stained with PerCP-labeled anti-CD8 antibody or an isotype control, fixed and permeabilized in Cytofix/Cytoperm buffer, and washed with Perm/Wash buffer. Intracellular staining was then performed with fluorescein isothiocyanate-labeled anti-IFN-γ antibody or anti-RANTES antibody (BD Pharmingen) and followed by analysis on a FACScalibur flow cytometer with CellQuest software (Becton Dickinson).

**Analysis of CTL ability to suppress HIV-1 replication.** A functional assay to evaluate the ability of CTL to suppress viral replication was performed as previously described (40). In brief, T1 cells were acutely infected with HIV-1 IIIB at a multiplicity of $10^{-2}$ 50% tissue culture infective doses per cell. The T1 cells were then cocultured in 24-well flat-bottom plates at a ratio of $5 \times 10^5$ cells to $1.25 \times 10^5$ CTL in 2 ml of medium. At the indicated time points, 1 ml of medium was removed for quantitative p24 antigen enzyme-linked immunosorbent assay and replaced with fresh medium.

## RESULTS

**Telomerase transduction preserves the replicative capacity of polyclonal CD8$^+$ T cells.** Ectopic telomerase transduction has been reported to prevent replicative senescence in primary CD8$^+$ T cells (18, 28). We tested the effect of hTERT transduction on the proliferation of early-passage polyclonal human CD8$^+$ T-cell lines derived from HIV-1-infected individuals (Fig. 1). Proliferation of the transduced and control (vector-transduced) cells progressively diverged over time, and whereas the doublings of the nontransduced cells plateaued after approximately 400 to 500 days of culture, the transduced cells continued to proliferate at a constant rate. On average, the control cells stopped proliferating after a mean of 20 ± 5 doublings over 589 ± 117 days, whereas the transduced cells continued proliferating beyond 800 days of follow-up (not shown). Telomerase activity, analyzed by the TRAP assay, was maintained in the transduced cell cultures but absent in the

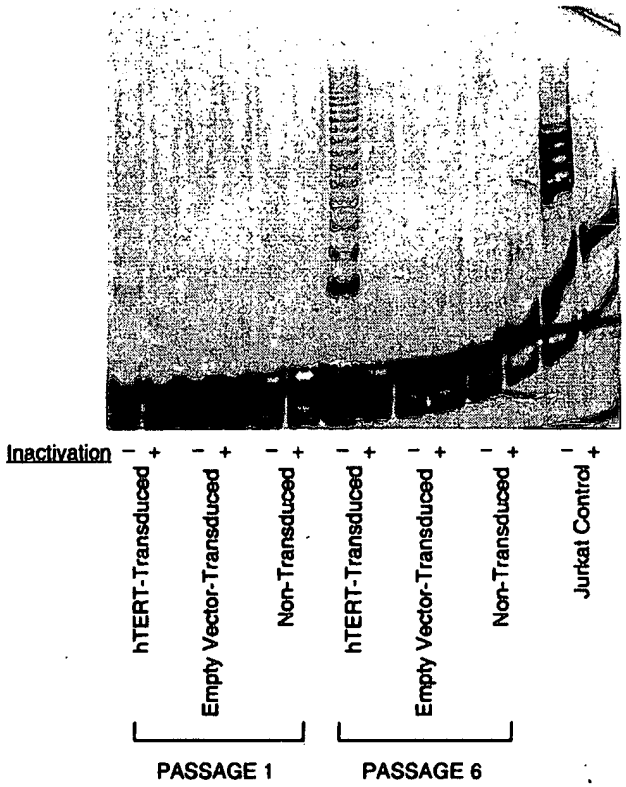


FIG. 2. Ectopic telomerase activity in hTERT-transduced CTL. Telomerase activity, as measured by the TRAP assay, was tested in extracts from hTERT-transduced and control CTL at 14 days after restimulation, when endogenous telomerase activity is quiescent. Telomerase activity was reflected by DNA laddering (Jurkat cell positive control). Heat-treated cellular extracts (to inactivate telomerase) served as negative controls. CTL (hTERT transduced, empty vector transduced, and nontransduced) from one passage after transduction (lanes 1 to 6) and six passages after transduction (lanes 7 to 12) were evaluated.

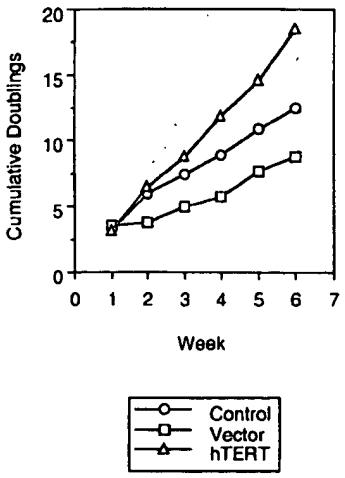


FIG. 3. Growth of hTERT-transduced CTL over repeated passages. After hTERT transduction, cell doublings were calculated after each passage of 1 week. Cumulative cell doublings over time are plotted for nontransduced, vector-transduced, and hTERT-transduced CTL clones.

control cells (not shown). These results extend findings on the antisenescence effects of telomerase on $CD8^+$ T cells from HIV-1-infected persons.

**Telomerase activity is maintained in hTERT-transduced HIV-1-specific CTL.** To specifically study the effects of telomerase transduction on HIV-1-specific $CD8^+$ T cells, we then transduced the human $CD8^+$ HIV-1-specific CTL clone 68A62, which recognizes an epitope in reverse transcriptase (39, 40). To verify successful transduction and expression of hTERT, we assayed these cells for telomerase activity at 14 days after restimulation (Fig. 2), a time point when endogenous telomerase activity had declined to undetectable levels. At the first passage after transduction, the hTERT-transduced cells already demonstrated significant activity, as seen by characteristic DNA laddering in a TRAP assay (Fig. 2, lane 1). By the sixth passage after transduction, telomerase activity had increased markedly (Fig. 2, lane 7), suggesting preferential expansion of cells ectopically expressing the transgene. It is worth noting that there was no experimental manipulation to enrich for transduced cells during passaging. Telomerase activity was absent in the negative control nontransduced (Fig. 2, lanes 5 and 11) and empty-vector-transduced (Fig. 2, lanes 3 and 9) cells at both passages analyzed. These results indicate that the CTL were successfully transduced with hTERT and suggest that transduction conferred a selective proliferative advantage.

**HIV-1-specific CTL transduced with hTERT exhibit enhanced proliferative capacity.** The proliferative capacity of CTL upon repeated stimulation in vitro dramatically decreases as they are serially passaged (Fig. 3 and unpublished observations). To determine whether introduction of telomerase had an effect on the growth of CTL, we followed their rate of expansion for multiple passages after transduction (Fig. 3). Immediately after transduction, hTERT-transduced and control CTL proliferated to similar degrees. However, with further passaging, the control CTL showed blunted levels of proliferation in comparison to the hTERT-expressing cells. The expansion of the cells still remained dependent upon stimulation (by anti-CD3 antibody and irradiated feeder cells) and IL-2, and their growth plateaued about 7 to 10 days after each restimulation (not shown). Thus, ectopic expression of telomerase in the CTL led to relative preservation of proliferative potential over time compared to that of untransduced cells, without evidence of transformation.

**Antigen-specific lytic function is preserved in hTERT-transduced but not nontransduced CTL.** To evaluate the effect of constitutive telomerase expression on the peptide-specific lytic function of CTL, killing of peptide-loaded target cells by chromium release assay was evaluated after each passage (Fig. 4). Whereas the level of killing by control CTL dropped steadily over time, cytolytic activity was maintained by hTERT-transduced CTL for approximately 10 weeks. In agreement with published observations on HIV-1-specific CTL, cytolysis by these CTL was mediated entirely through the calcium-dependent proteolytic pathway and not through apoptosis (not shown). These data suggest that telomerase activity contributed to the preservation of proteolytic cytolytic function in these cells over time.

**Loss of lytic function in nontransduced CTL is not due to**

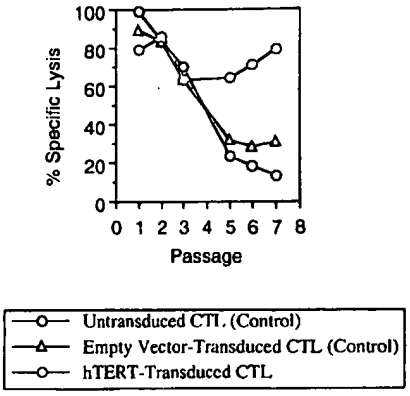


FIG. 4. Antigen-specific lytic activity of hTERT-transduced CTL over repeated passages. After each passage, control and hTERT-transduced CTL were evaluated for the ability to kill peptide-loaded target cells (the T1 cell line matched at HLA A2, loaded with the IV9 peptide) as measured by a standard chromium release assay. Results obtained at an effector-to-target cell ratio of 5:1 are shown; similar results were obtained at lower ratios. Target cell killing was peptide specific in all cases (not shown). These data are representative of two independent transduction experiments. In both experiments, cytolytic activity in the hTERT-transduced CTL waned after about 10 weekly passages (not shown).

**overgrowth of nonspecific cells.** To exclude the possibility that loss of killing activity in the nontransduced cells was due to overgrowth of non-reverse-transcriptase-specific cells lacking the appropriate T-cell receptor (TCR), the cultures were analyzed by peptide-MHC tetramer staining (Fig. 5). This analysis indicated that both hTERT-transduced (100%) and nontransduced (96%) CTL expressed the TCR recognizing the HLA A2-restricted epitope ILKEPVHGV, although the intensity of staining for both CD8 and the TCR was lower in the nontransduced cells. Thus, the waning of cytolytic activity in the control CTL was not due to dilutional loss of CTL with continued passaging.

**IFN-γ and RANTES production is relatively unaffected by hTERT transduction of CTL.** We evaluated the ability of CTL to produce cytokines associated with important effector functions, namely, IFN-γ, whose synthesis is induced by antigenic stimulation (19), and RANTES, which is presynthesized and stored in cytolytic granules of CTL at rest (32). By using intracellular staining, we evaluated telomerase-transduced and control CTL for the ability to generate IFN-γ in response to stimulation (Fig. 6) and RANTES at baseline (Fig. 7). Production of both of these cytokines was similar, regardless of telomerase transduction status. IFN-γ staining intensity was induced 4.3-fold in hTERT-transduced CTL, compared to 4.5- and 5.7-fold in control CTL. RANTES in CTL at rest produced mean fluorescence intensities of 17.0 for hTERT-transduced cells and 13.3 and 15.5 for control cells. Thus, telomerase transduction did not appear to markedly affect production of these cytokines by CTL, in contrast to the effects on cytolytic function.

**Telomerase transduction enhances the antiviral function of HIV-1-specific CTL.** Finally, we evaluated the antiviral function of CTL in coculture with acutely HIV-1-infected cells (Fig. 8). Control nontransduced CTL decreased HIV-1 replication about 10-fold, similar to previously published studies with this clone (40, 41). However, hTERT-transduced CTL were an order of magnitude more efficient, exerting about 100-fold suppression of viral replication. Thus, ectopic telomerase activity appears to preserve or augment the antiviral function of CTL in parallel with its effects on cytolytic function. These observations are consistent with the central role of cytolysis in the ability of CTL to suppress HIV-1 replication (40).

## DISCUSSION

T cells differ from most human somatic cells in that they express telomerase transiently during differentiation and activation (6, 10, 16, 35). Nevertheless, the level of telomerase activity induced in memory T cells declines with repeated stim-

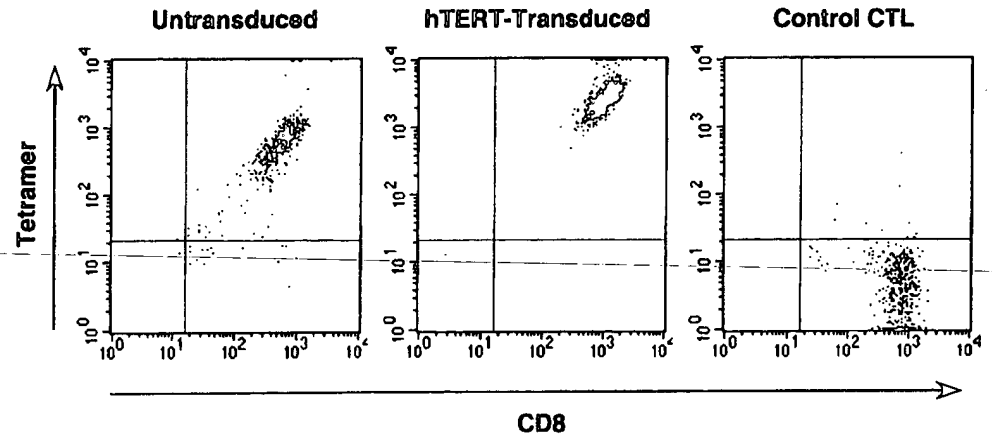


FIG. 5. TCR expression by hTERT-transduced CTL. Control and hTERT-transduced CTL passaged for 6 weeks after transduction were assessed for expression of the appropriate TCR by flow cytometric analysis of CD8 and TCR expression by antibody and peptide-MHC tetramer binding. Untransduced CTL were 96% positive for CD8 and TCR, and hTERT-transduced CTL were 100% positive. The mean fluorescence intensities of staining of CD8 were 610 and 1,130, and those of the TCR were 756 and 2,951, respectively. A parallel specificity control (a CTL clone recognizing a different epitope) is also shown; these cells were 97% CD8 positive and TCR negative by tetramer staining, with a CD8 mean fluorescence intensity of 767.

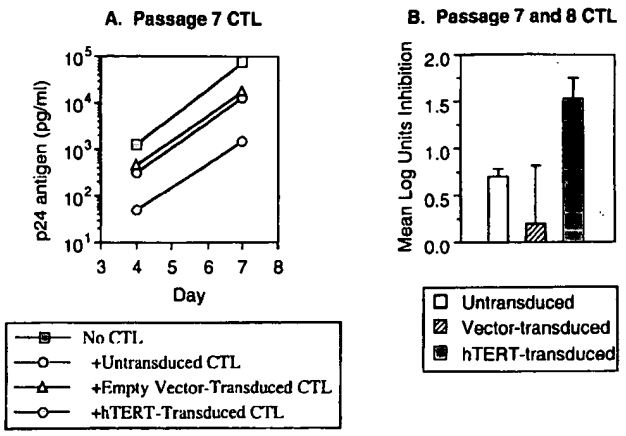


FIG. 8. Suppression of HIV-1 replication by hTERT-transduced CTL. Control and hTERT-transduced CTL passaged for 7 or 8 weeks after transduction were cocultured with acutely HIV-1-infected T1 cells ($1.25 \times 10^5$ CTL with $5 \times 10^5$ T1 cells infected with HIV-1 IIIB at $10^{-2}$ 50% tissue culture infective doses per cell), and viral replication was measured by serial quantitative p24 antigen enzyme-linked immunosorbent assays. (A) Viral replication in the absence or presence of CTL after seven passages is plotted. (B) Suppression of HIV-1 replication after 7 days of coculture is plotted. The bars represent the means of independent experiments with CTL after 7 and 8 weeks of passage, and the error bars represent 1 standard deviation.

cytolytic effector function of CTL and that the defect is at least partially preventable by hTERT transduction. Telomere shortening and replicative senescence may therefore be important contributing factors in the inability of CTL to contain HIV-1 infection in vivo, which is a topic of intense discussion (4, 22, 23). Consistent with this hypothesis, HIV-1-specific CTL in vivo have been found to contain reduced levels of perforin compared to cytomegalovirus-specific CTL in the same persons, suggesting a specific defect in the lytic pathway (2). Intriguingly, a recent study has shown that long-term nonprogressing HIV-1 infection appears to be associated with perforin production and proliferative capacity of HIV-1-specific CTL and that these are linked (25). Finally, the decrease in CD8 and/or TCR expression we noted in the nontransduced CTL could play a role in diminished antiviral function by reducing the sensitivity of CTL for their target cells. It has been noted that some HIV-1 epitopes may be presented by infected cells at a limiting concentration (29, 39), and a decrease in TCR and CD8 expression could therefore have a significant impact on infected cell recognition by CTL. In sum, chronic turnover and shortened telomeres in HIV-1-specific CTL could thus lead to diminished antiviral activity in vivo through one or a combination of these mechanisms.

In contrast to its effects on cytolytic and antiviral functions, telomerase transduction did not markedly affect the ability of CTL to produce two important cytokines. Production of both IFN-γ, which is induced by antigenic exposure (19), and RANTES, which is constitutively produced but stored in the cytolytic granules for release upon antigenic exposure (32), was maintained in the absence of ectopic telomerase activity. This suggests either that telomerase transduction of presenescent CTL cannot prevent defects in cytokine production or, more likely, that production of these cytokines does not wane as dramatically with senescence as lytic activity. Although suppression of HIV-1 replication by CTL in vitro has been shown to occur through cytokine (including chemokine)- and cytolysis-mediated pathways (11, 40), the cytolytic activity of CTL appears to add several orders of magnitude of inhibition over that of cytokines alone (40). A preferential diminution of cytolytic function by senescence would therefore be predicted to result in loss of antiviral activity, consistent with our finding that suppression of HIV-1 by CTL is enhanced by telomerase transduction. Importantly, because the most widely used new technologies for CTL quantitation in vivo (9) rely on detection of IFN-γ responses or direct binding of the TCR, they do not reflect the lytic or antiviral activity of these CTL. As a result, these assays may fail to detect dysfunction induced by senescence.

The lytic ability of the transduced cells did eventually wane after about 10 weeks of continuous passaging. This was in contrast to the observation of Rufer et al., who found that hTERT-transduced $CD8^+$ T cells became essentially immortal (28). The reason for this difference is unclear, but it could be related to the fact that the HIV-1-specific CTL were already nearly senescent at the time of transduction. Moreover, others have found that even telomerase-transduced T cells may still be subject to exhaustion (24). The T cells used in our study were originally cloned from the blood of a chronically HIV-1-infected individual and passaged for a long time in vitro and were therefore likely to be closer to senescence than cells previously studied by other groups. Further study is required to confirm the etiology of this difference.

In conclusion, ectopic expression of hTERT in HIV-1-specific CTL leads not only to enhancement of the replicative capacity of these cells but also to preservation of cytolytic effector function and antiviral activity. These findings have ramifications for our understanding of the consequences of chronic CTL turnover in HIV-1-infected individuals and suggest that cellular immune dysfunction is at least partially preventable by telomerase transduction. In sum, these data suggest that telomerase transduction is a potential novel experimental approach by which to dissect the mechanisms of immune dysfunction induced by chronic HIV-1 infection or other conditions under which chronic turnover leads to T-cell senescence.

## ACKNOWLEDGMENTS

R.B.E. and O.O.Y. contributed equally to this work.

This work was funded by National Institutes of Health grants RO1 AI43203 (O.O.Y.), R21 AI47665 (R.B.E.), RO1 AI35040 (R.B.E.), and F31 AG05920 (M.D.). IL-2 was provided by the National Institutes of Health AIDS Research and Reference Reagent Repository.

We thank Bruce D. Walker for providing clone 68A62 and Geron Corporation for providing the hTERT construct vector.

## REFERENCES

1. **Allsopp, R. C., H. Vaziri, C. Patterson, S. Goldstein, E. V. Younglai, A. B. Futcher, C. W. Greider, and C. B. Harley.** 1992. Telomere length predicts replicative capacity of human fibroblasts. Proc. Natl. Acad. Sci. USA **89:** 10114–10118.
2. **Appay, V., D. F. Nixon, S. M. Donahoe, G. M. Gillespie, T. Dong, A. King, G. S. Ogg, H. M. Spiegel, C. Conlon, C. A. Spina, D. V. Havlir, D. D. Richman, A. Waters, P. Easterbrook, A. J. McMichael, and S. L. Rowland-Jones.** 2000. HIV-specific $CD8^+$ T cells produce antiviral cytokines but are impaired in cytolytic function. J. Exp. Med. **192:**63–75.
3. **Bestilny, L. J., M. J. Gill, C. H. Mody, and K. T. Riabowol.** 2000. Accelerated replicative senescence of the peripheral immune system induced by HIV infection. AIDS **14:**771–780.

# Constitutive Human Telomerase Reverse Transcriptase Expression Enhances Regenerative Properties of Endothelial Progenitor Cells

Satoshi Murasawa, MD, PhD; Joan Llevadot, MD; Marcy Silver, BS; Jeffrey M. Isner, MD†; Douglas W. Losordo, MD; Takayuki Asahara, MD, PhD

***Background***—The regulatory molecule for cell life span, telomerase, was modified by human telomerase reverse transcriptase (hTERT) gene transfer to investigate its effect on regenerative properties of endothelial progenitor cells (EPCs) in neovascularization.

***Methods and Results***—Telomerase activity was enhanced in hTERT-transduced EPCs (Td-TERTs) (1.2-fold versus no transduced EPCs [no-Td] and 1.2-fold versus GFP-transduced EPCs [Td/GFPs] at day 8; 5.2-fold versus no-Td and 4.8-fold versus Td/GFP at day 21, respectively) Mitogenic capacity in Td/TERTs exceeded that in Td/GFPs at day 8 ($0.62\pm0.02$ versus $0.53\pm0.01$, respectively; $P<0.01$). Vascular endothelial growth factor–induced cell migration in EPCs was markedly enhanced by hTERT overexpression (Td/TERTs versus Td/GFPs, $292\pm12$ versus $174\pm6$ cells, respectively; $P<0.01$). hTERT overexpression has rescued EPCs from starvation-induced cell apoptosis, an outcome that was further enhanced in response to vascular endothelial growth factor. The colony appearance of totally differentiated endothelial cells (tdECs) was detected before day 30 only in Td/TERT, whereas no tdEC colonies could be detected in both Td/GFPs and no-Tds. Finally, we investigated in vivo transplantation of heterologous EPCs. Td/TERTs dramatically improved postnatal neovascularization in terms of limb salvage by 4-fold in comparison with that of Td/GFPs; limb perfusion was measured by laser Doppler ($0.77\pm0.10$ versus $0.47\pm0.06$; $P=0.02$), and capillary density ($224\pm78$ versus $90\pm40$ capillaries/mm$^2$; $P<0.01$).

***Conclusions***—These findings provide the novel evidence that telomerase activity contributes to EPC angiogenic properties; mitogenic activity, migratory activity, and cell survival. This enhanced regenerative activity of EPCs by hTERT transfer will provide novel therapeutical strategy for postnatal neovascularization in severe ischemic disease patients. (***Circulation.* 2002;106:1133-1139.**)

**Key Words:** telomerase ■ gene therapy ■ stem cells, endothelial ■ angiogenesis ■ ischemia

The plasticity of stem and progenitor cells is attracting the attention to regenerative application to many inherited and acquired diseases. The regenerative potential of bone marrow–derived endothelial progenitor cells (EPCs)[1–5] has been previously demonstrated in animal models of myocardial[6] and limb[7] ischemia, via ex vivo expansion and incorporation into foci of neovascularization. Physiological evidence of neovascular function in these preclinical animal models disclosed an improvement in myocardial function or a high rate of limb salvage. Despite promising applications for tissue regeneration, the limited endogenous pool, the possible functional impairment associated with a variety of physiological and pathological phenotypes on clinical patients, and the finite replicative feature of EPCs for ex vivo expansion constitute potentially important liabilities for autologous transplantation. We hypothesized that gene transfer can be used to achieve phenotype modulation of EPCs to overcome this issue. Very recently, our laboratory has determined the impact of vascular endothelial growth factor (VEGF) gene transfer on certain properties of EPCs in vitro and the consequences of VEGF EPC transfer on neovascularization in vivo.[8]

Most somatic cells of humans and other mammals undergo a finite number of cell divisions, ultimately entering a nondividing state termed senescence.[9–11] Loss of telomerase activity has been suggested to constitute the molecular clock that triggers cellular senescence.[12,13] In contrast to somatic cells, true stem cells and germline cells highly express the

Received April 8, 2002; revision received June 11, 2002; accepted June 11, 2002.

From the Department of Medicine (Vascular Medicine, Cardiology, Cardiovascular Research), St Elizabeth's Medical Center, Tufts University School of Medicine (S.M., J.L., M.S., J.M.I., D.W.L., T.A.), Boston, Mass; Stem Cell Translational Research, Kobe Institute of Biomedical Research and Innovation/Riken Center for Developmental Biology (S.M., T.A.), Kobe, Japan; Department of Physiology, Tokai University School of Medicine (T.A.), Kanagawa, Japan.

†Deceased.

Correspondence to Douglas W. Losordo, MD, or Takayuki Asahara, MD, PhD, St Elizabeth's Medical Center, 736 Cambridge St, Boston, MA 02135. E-mail douglas.losordo@tufts.edu or asa777@aol.com



*Circulation* is available at http://www.circulationaha.org

DOI: 10.1161/01.CIR.0000027584.85865.B4

catalytic subunit of telomerase (human telomerase reverse transcriptase [hTERT]),[13–16] thus maintaining telomerase activity and full replication of telomeric DNA; these cells (by definition) are thereby able to divide indefinitely.[17] Although demonstrating regenerative potentials for vascular development, EPCs are not pluripotent, self-renewing stem cells, but rather lineage-committed progenitors, and are thus subject to a Hayflick life span[18] via replicative senescence. Accordingly, we have deduced that constitutive expression of hTERT might induce delay in senescence and recover/enhance regenerative properties of EPCs. Ectopic expression of the hTERT gene has been investigated as a means to bypass senescence; indeed, this strategy has been used successfully to impart replicative immortality to fibroblasts and retinal pigment epithelial cells[19] without converting either to a transformed neoplastic phenotype.[20,21] The immortalized blood vessel–derived endothelial cells (ECs) similarly exhibited neither evidence of malignant transformation nor loss of functional and morphogenetic characteristics of the parental cells.[22] Such hTERT-transduced (Td-hTERT) EC lines appeared more resistant to programmed cell death, exhibited a survival advantage beyond replicative senescence,[22] and had improved NO production compared with that of control senescent cells.[23]

These findings have encouraged consideration of potential therapeutic applications of hTERT gene transfer to achieve functional improvement in EPCs through delay in senescence and recovering/enhancing regenerative properties of EPCs.

## Methods

### EPC Culture and Gene Transfer

Total peripheral blood mononuclear cells were isolated from human volunteers by density-gradient centrifugation. After 4 days in culture, nonadherent cells were removed by washing with PBS, new media was applied, and the culture was maintained through day 7 or later.[24] In the culture of EPCs after day 7, reseeding was performed once a week. Both Ad/hTERT (Ad5CMVe/β-actin pro/hTERT ΔE3) and Ad/GFP (Ad5CMV/GFP ΔE3) were provided by Geron Inc (Menlo Park, Calif). Briefly, the recombinant adenoviruses were constructed by homologous recombination between the parental virus genome and the expression cosmid cassette or shuttle vector as described.[25,26] Day-7 cultured EPCs were transduced with 500 MOI of Ad/hTERT or Ad/GFP in endothelial cell growth media (EGM-2) supplemented with 1% fetal bovine serum for 3 hours, and the next day, transduced EPCs were reseeded or assayed.

### Reverse Transcription–Polymerase Chain Reaction

Cells with or without adenovirus gene transduction were lysed in RNA lysis buffer (Ambion). RNA was extracted by use of an RNA extraction kit (Ambion). DNAase digestion was performed after RNA extraction. The reverse transcription–polymerase chain reaction (RT-PCR) was performed by a system according to the manufacturer (Clontech). The primers for RT-PCR in the hTERT gene were follows: sense, CACCTCACCTCACCCACgCgAAA; antisense, CCAAAgAgTTTgCgACgCATgTT.

### Telomeric Repeat Amplification Protocol Assay

EPCs were washed with PBS and $1\times10^5$ cells were lysed in 200 μL of 3[(3-cholamidopropoyl)-dimethylammonio]-1-propane-sulfonate (CHAPS) lysis buffer (10 mmol/L Tris-HCl at pH 7.5, 1 mmol/L $MgCl_2$, 1 mmol/L EGTA, 0.1 mmol/L benzamidine, 5 mmol/L β-mercaptoethanol, 0.5% w/v CHAPS, 10% w/v glycerol). The homogenate was incubated on ice for 30 minutes and centrifuged at 12 000*g* for 30 minutes. An aliquot of 2 μL of this supernatant (1000 cell equivalents) was used for PCR amplification to detect the telomerase products. Telomerase products were amplified with the downstream reverse primer (RP; 5′ GCGCGG $(CTTACC)_3$ CTA-ACC 3′) and the upstream primer telomerase substrate (TS; 5′ AATCCGTCGAGCAGAGTT 3′); 293-cell extract was used for positive control.

### SA-β-Gal Activity Assay

EPC senescence was investigated by senescence-associated β-galactosidase (SA-β-Gal) activity assay described previously.[27]

### Proliferation and Migration Assays

Proliferative activity of transduced EPCs was evaluated using the MTS assay (MTS Assay, Promega).[24] EPC migration was evaluated using a modified Boyden chamber assay.[24]

### Apoptosis Assay

To detect the frequency of cellular apoptosis, fluorescence-labeled Annexin-V-FLUOS staining of transduced EPCs was performed according to manufacturer's instructions (Roche Molecular Biochemicals).[28]

### EPC Differentiation Colony Assay

Transduced EPCs were cultured as described above and reseeded once per week. Colony appearance of totally differentiated ECs (tdECs) was studied under phase contrast microscopy 3 days per week. Established colonies were evaluated as tdECs by use of assays for 1,1′-dioctadecyl-3,3,3′,3′-tetramethylindocarbocyanine perchlorate (acLDL-DiI) incorporation and Matrigel tube formation. Incorporation of acLDL-DiI typically appears less intense in tdECs (stain moderately within 1 hour with 20 μg/mL acLDL-DiI) than in the less differentiated EPCs (stain strongly within 30 minutes with 5 μg/mL acLDL-DiI). Non-EC—including fibroblasts, myoblasts, and epiblasts—do not incorporate acLDL. Within 12 hours, tdECs form complete capillary-like tubes in Matrigel (Becton Dickinson Labware).[1,28]

### Murine Hindlimb Ischemia Model

The impact of EPC administration on therapeutic neovascularization was investigated in a murine model of hindlimb ischemia, by use of athymic nude or severe combined immunodeficient mice.[29–31] Athymic nude mice (Jackson Labs, Bar Harbor, Maine), age 8 to 10 wks and weighing 17 to 22 g, were anesthetized with 160 mg/kg pentobarbital intraperitoneally for operative resection of one femoral artery, and subsequently for laser Doppler perfusion imaging (LDPI; Lisca).[28,32,33] Immediately before euthanasia, mice were injected with an overdose of pentobarbital. One day after operatively induced hindlimb ischemia, the athymic nude mice, in which angiogenesis is characteristically impaired,[34] received an intravenous injection of $1.5\times10^4$ culture-expanded EPCs transduced with Ad/hTERT (Td/hTERT) or Ad/GFP (Td/GFP). Tissue sections were stained for alkaline phosphatase by use of indoxyltetrazolium to detect capillary ECs, as previously described[29] and were then counterstained with eosin.

## Results

### Time Course of hTERT Overexpression After Adenoviral Transduction

RT-PCR was performed to evaluate the hTERT expression level after adenoviral transduction. Endogenous hTERT was observed only in day-10 nontransduced EPCs (no-Td). On the other hand ectopic hTERT was highly expressed at day 10, 3 days after Ad/hTERT transduction, and was gradually reduced during cultivating EPCs. Reseeding was performed days 4 and 7 after isolation and once a week after day 7. (Figure 1).

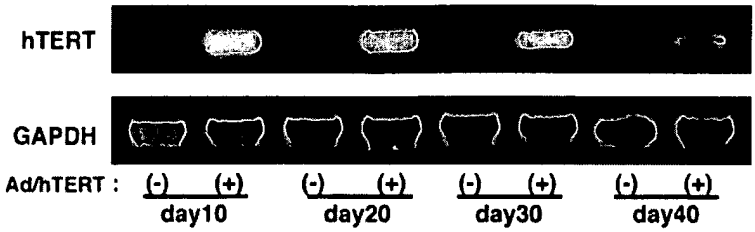


**Figure 1.** Expression of hTERT mRNA level. RNA samples from EPCs with or without Ad/hTERT were analyzed by RT-PCR for the expression of hTERT. GAPDH served as internal standard. (+) indicates EPCs transduced with Ad/hTERT at day7; (−), EPCs without adenoviral transduction.

### Telomerase Activity After hTERT Overexpression

EPC gene modification was performed using adenovirus-encoding hTERT or green fluorescent protein (GFP; Ad/hTERT and Ad/GFP, respectively). Cultured EPCs, transduced on day 7 with Ad/hTERT and Ad/GFP (Td/hTERT or Td/GFP, respectively), as well as no-Tds, were assayed for telomerase activity at 1, 7, and 14 days after transduction (days 8, 14, and 21 in culture, respectively). Telomerase activity appeared robust in no-Td EPCs at day 8 but was dramatically reduced by days 14 and 21 (Figure 2A). After gene transfer, telomerase activity was enhanced in Td/hTERT EPCs (1.2-fold versus no-Td and 1.2-fold versus Td/GFP at day 8; 1.5-fold versus no-Td and 1.2-fold versus Td/GFP at day 14; 5.2-fold versus no-Td and 4.8-fold versus Td/GFP at day 21) (Figure 2B).

### SA-β-Gal Activity in EPCs

The impact of hTERT expression on EPC senescence was evaluated by SA-β-Gal activity assay to confirm the result of telomerase activity. At day 8, SA-β-Gal–positive cells were equally rare among no-Td, Td/hTERT, and Td/GFP EPCs (0.13%±0.02 versus 0.07%±0.01 versus 0.27%±0.02; $P$=NS). At day 14, the proportion of SA-β-Gal positive cells was increased (≈5%) in no-Td and Td/GFP EPCs; among Td/hTERT, however, a very low proportion of senescent cells (no-Td versus Td/hTERT versus Td/GFP, 5.13%±0.30 versus 0.20%±0.02 versus 5.0%±0.30; $P$<0.01) were observed. By day 21, the proportion of SA-β-Gal–positive cells in no-Td and Td/GFP EPCs was markedly increased versus Td/hTERT (no-Td versus Td/hTERT versus Td/GFP, 25.2%±0.4 versus 5.4%±0.2 versus 24.2%±0.5; $P$<0.01)

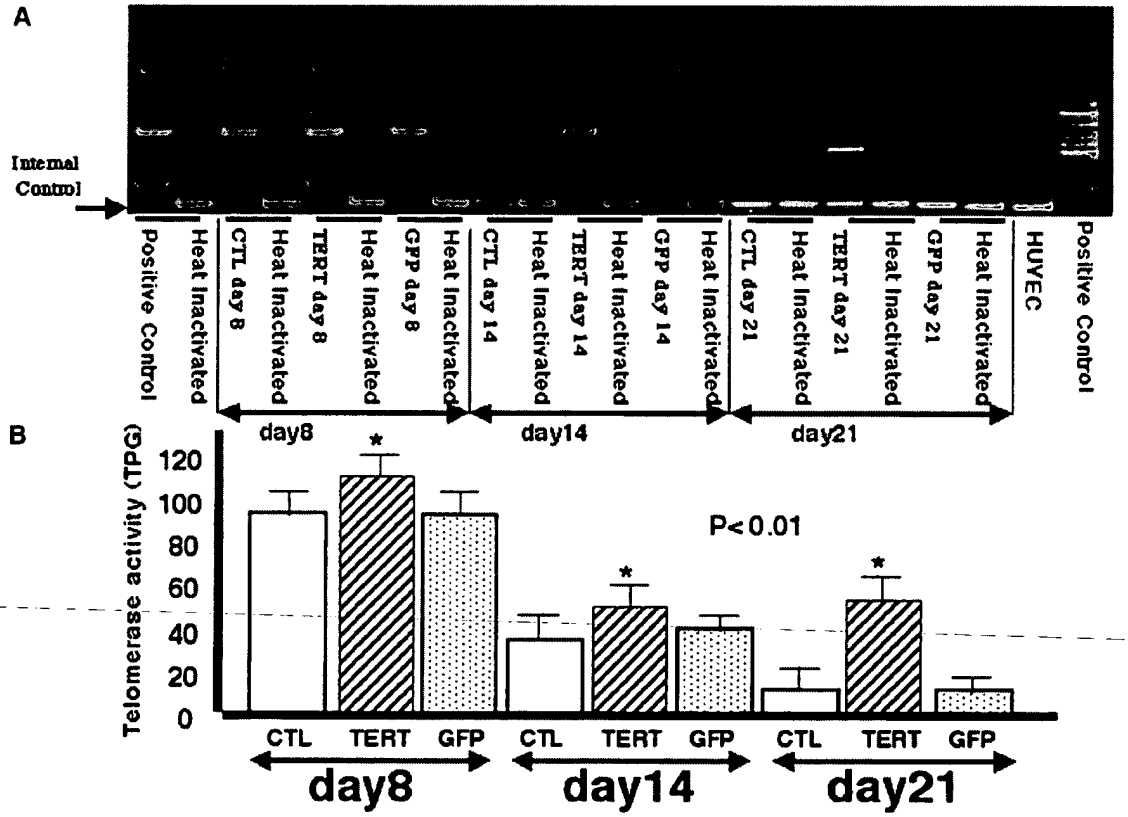


**Figure 2.** Telomerase activity in Td/hTERT, Td/GFP, and no-Td EPCs. EPCs were transduced on culture day 7 with adenovirus-encoding hTERT or GFP (Td/hTERT or Td/GFP, respectively) or no vector (no-Td). EPCs from 1, 7, and 14 days after transduction (culture days 8, 14, and 21, respectively) were used for telomerase activity assay. A, An aliquot of 2 μL of this supernatant (1000 cell equivalents) was used for PCR amplification to detect the telomerase products. Positive control indicates cell extract from positive control; heat inactivated, heat inactivated sample; and HUVEC, cell extract from human umbilical vein endothelial cell. B, Quantification of telomerase activity was performed to identify the total product generated (TPG) by densitometry of the digitized image (CTL indicates no-Td; TERT, Td/hTERT; and GFP, Td/GFP).

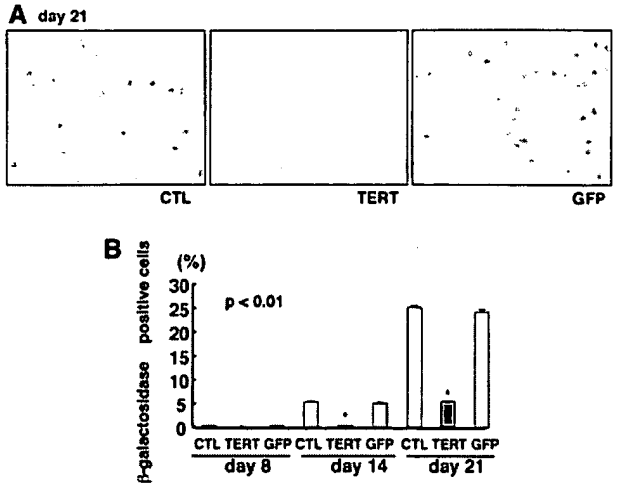


**Figure 3.** Senescence assay. A, EPC senescence was evaluated by acidic-β-gal staining. Representative photomicrographs show SA-β-gal–positive cells (blue) in no-Tds, Td/hTERTs, and Td/GFPs at day 21. B, Quantification of β-gal–positive cells was performed in no-Tds, Td/hTERTs, and Td/GFPs at days 8, 14, and 21, respectively. The number of blue cells was manually counted from a total of 2000 cells. By day 21, the proportion of SA-β-Gal–positive cells in no-Tds and Td/GFPs was markedly increased versus Td/hTERTs. A statistically significant reduction in β-gal–positive (senescent) cells was documented among Td/hTERT EPCs at days 14 and 21.

(Figure 3A and 3B). The results suggest that hTERT expression facilitates delay in senescence.

## Effect of hTERT Overexpression on EPC Differentiation

The finding of enhanced EPC differentiation also supports the contribution of hTERT overexpression. During long-term follow-up, colonies of tdEC were observed at day 30 only in Ad/TERT-transduced EPCs, whereas no-Td and Td/GFP cells detached before day 30, yielding no colonies in either group at this time point (Figure 4A). Incorporation of acLDL-DiI was evaluated to distinguish functional difference between tdECs and undifferentiated cells. The centrally located tdECs were identified by typically less intense uptake of acLDL-DiI versus the peripherally located, intensely stained, undifferentiated cells (Figure 4B). Colonies of tdECs formed sheetlike monolayers; the maximum number of colonies averaged 38 per 35-mm well (Figure 4C). The tdECs also formed capillary-like structures when reseeded in Matrigel (Figure 4D). The tdECs were equivalent to control differentiated ECs (human umbilical vein ECs and human microvascular ECs), both in terms of capillary-like response in Matrigel and of FACS analysis of endothelial surface molecule expression (data not shown). Follow-up (40 days) of Td/hTERT and Td/GFP EPCs disclosed no evidence of neoplastic transformation, including neither loss of contact inhibition nor unchecked cellular proliferation.

## EPC Mitogenic and Migratory Activity After hTERT Overexpression

The impact of hTERT overexpression on regenerative potential was apparent from analysis of angiogenic profiles in hTERT overexpressing EPCs. MTS assay demonstrated that mitogenic potential after Td/hTERT transduction exceeded that in Td/GFP at day 8 ($0.62\pm0.02$, $0.53\pm0.01$, respectively; $P<0.001$) (Figure 5A). Similarly, migratory activity in EPCs after hTERT transduction was analyzed in a modified Boyden chamber assay. VEGF-induced cell migration was markedly enhanced by hTERT overexpression (Td/hTERT versus Td/GFP, $292\pm12$ versus $174\pm6$ cells/4 fields, respectively; $P<0.001$) (Figure 5B).

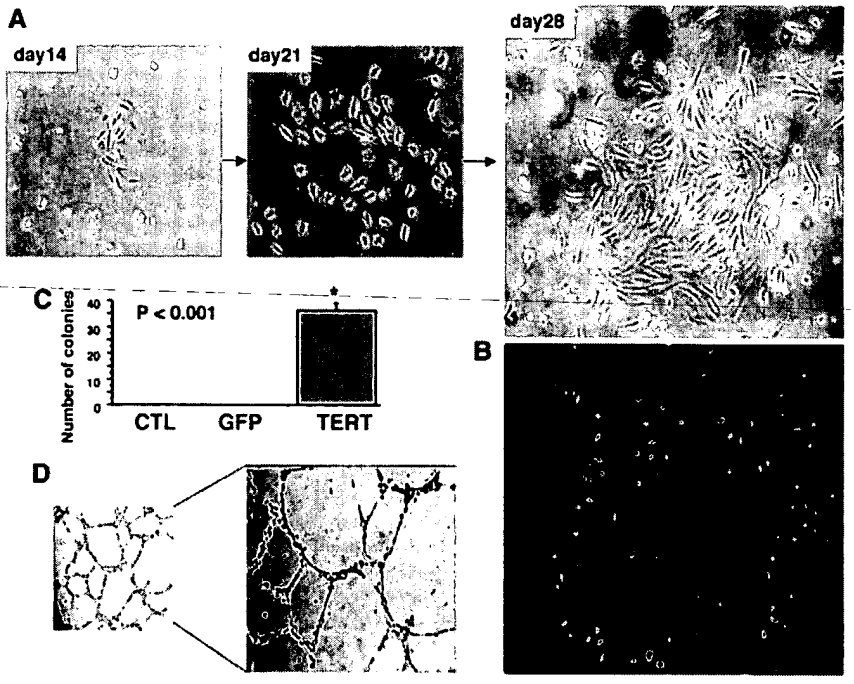


**Figure 4.** Assay of EPC differentiation. A, The colony appearance of tdECs was detected up to day 30 only in Ad/TERT-transduced EPCs. Upper panels show phase-contrast photomicrographs of the colony appearance of tdECs. B, acLDL-DiI incorporation: undifferentiated EPCs at the perimeter incorporated more acLDL-DiI than centrally located tdECs. The photo was taken 1 hour after adding acLDL-DiI. C, Number of colonies consisting of tdECs at day 30. Maximum number of colonies was m=38 per 35-mm well. Colonies were detected only in Td/hTERT culture dishes. $P<0.001$ vs Td/GFP and no-Td. D, Representative findings of tube formation assay. At day 30, $5\times10^4$ tdECs were seeded on Matrigel-coated plates. The EGM-2 media was supplemented with VEGF and incubated at 37°C for 12 to 24 hours. Tube formation was imaged by use of an inverted phase contrast microscope. Photos were taken 12 hours after reseeding. Right panel is a higher magnification of the left panel.

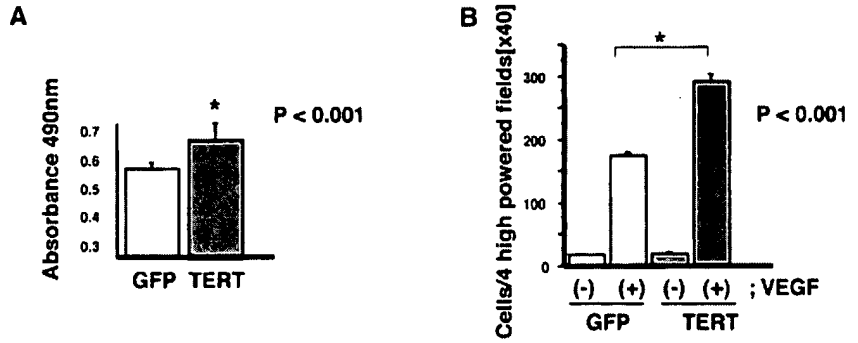


**Figure 5.** In vitro analyses after EPC transduction. A, Proliferative activity assay at day 8. The increase in mitogenic response of Td/hTERT was statistically significant in comparison with Td/GFP ($P<0.001$ vs Td/GFP). (TERT indicates Td/hTERT; GFP, Td/GFP) B, Migratory activity assay at day 8. Migratory effect induced by VEGF was statistically increased in Td/hTERT compared with Td/GFP ($P<0.001$ vs Td/GFP).

### EPC Survival After hTERT Transduction

The effect of hTERT modulation on EPC resistance to apoptosis was also evaluated. Immunofluorescent staining with Annexin-V and Hoechst33342 established that starvation-induced EPC apoptosis was markedly reduced after hTERT gene transfer. MTS assay (shown in Figure 5A) also supported these results. This outcome was amplified after VEGF administration (Figure 6).

### Physiological Impact In Vivo After Transplantation of hTERT-Transduced EPCs

Given the impact on regenerative features, EPC transplantation was performed to assess the corresponding physiological impact in vivo after hTERT gene modification. After 1-week ex vivo expansion, $1.5\times10^4$ human EPCs were transduced with Ad/TERT or Ad/GFP and administered intravenously to athymic nude mice with unilateral hindlimb ischemia (n=18 each). Compared with mice transplanted with Td/GFP, mice transplanted with Td/TERT demonstrated enhanced perfusion measured by LDPI ($0.77\pm0.10$ versus $0.47\pm0.06$ in arbitrary units measured by LDPI; $P=0.02$) (Figure 7B). The physiological relevance of this finding was underscored by the fact that salvage of the ischemic limb was significantly improved among mice transplanted with Td/TERT versus Td/GFP ($P<0.01$) (Figure 7A). Capillary density, evaluated in histologic sections retrieved at day 28 from ischemic hindlimb muscle, was markedly increased in mice receiving Td/TERT versus Td/GFP ($224\pm78$ versus $90\pm40$ capillaries/mm$^2$; $P<0.01$) (Figure 7D). Animals treated with Td/TERT or Td/GFP EPCs disclosed no evidence of neoplastic transformation.

## Discussion

We have challenged the otherwise inevitable reduction of telomerase activity in human EPCs by performing gene transfer to achieve constitutive expression of hTERT in these somatic progenitor cells. Constitutive expression of hTERT

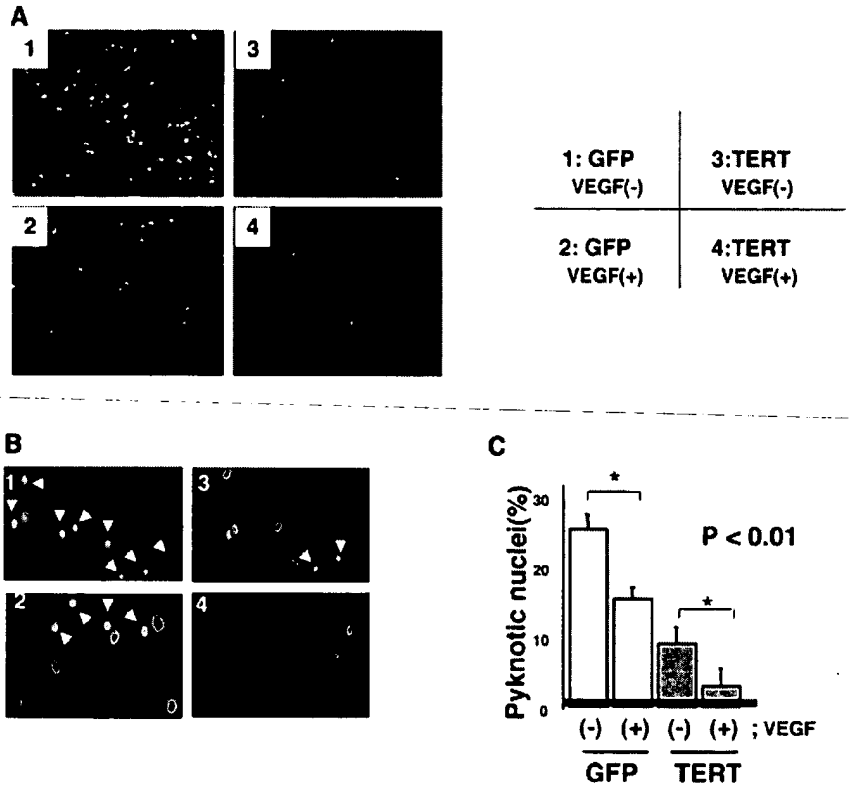


**Figure 6.** Apoptosis assay. A, Representative images show cell survival effects as a function of hTERT transduction and VEGF administration. Double staining was performed with Annexin-V (green) and propidium iodide (red). Day-7 cultured EPCs were transduced with hTERT or GFP, depleted of serum for 24 hours, and stimulated with 100 ng/mL of VEGF or vehicle. Evidence of apoptosis by staining for Annexin -V, propidium iodide, or both is reduced in TERT-EPCs. This outcome was amplified after VEGF administration. B, Representative images show cell survival effects by use of Hoechst33342 staining. Numbers on figures correspond to numbers indicated on accompanying table. The numbers of pyknotic nuclei identified by Hoechst-positive staining are reduced among TERT-EPCs. This outcome was amplified after VEGF administration. C, Quantitative analysis of VEGF-induced EPC survival by counting pyknotic nuclei stained by Hoechst33342. VEGF induced cell survival, and hTERT enhanced cell survival effect ($P<0.01$, VEGF-Td/GFP vs VEGF-Td/hTERT).

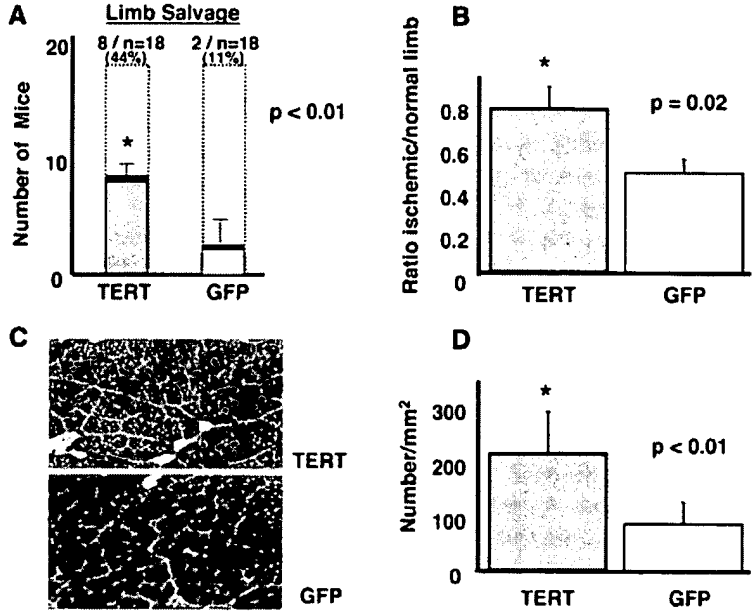


**Figure 7.** Therapeutic efficiency of Td/hTERT and Td/GFP EPCs in murine model of hindlimb ischemia. All data reflect analyses performed 28 days after administration of transduced EPCs. A, Impact on hindlimb integrity. Administration of Td/hTERT increased limb salvage (ie, neither toe nor limb necrosis) compared with that of controls transduced with a reporter (GFP) gene ($P<0.01$ Td/TERT vs Td/GFP). B, LDPI performed at day 28. Compared with mice transplanted with Td/GFP, mice transplanted with Td/TERT demonstrated enhanced perfusion measured by LDPI ($0.77\pm0.10$ vs $0.47\pm0.06$ in arbitrary units measured by LDPI; $P=0.02$) C, Histologic evidence of neovascularization in ischemic hindlimb. Representative photomicrographs of capillaries in tissue sections from muscle of ischemic legs stained with alkaline phosphatase. D, Quantification of capillary density. The extent of neovascularization was assessed by measuring capillary density in light microscopic sections prepared from muscles of ischemic hindlimbs. Capillary density was significantly greater in hindlimbs of mice receiving Td/hTERT ($P<0.01$ vs Td/GFP).

led to conservation of telomerase activity and delay in senescence, as well as enhanced EPC regenerative properties, including mitogenesis, migration, and EPC survival. EPC differentiation colony assay also disclosed distinct consequences of hTERT transduction of EPCs. Differentiated colonies appeared only among hTERT-expressing EPCs. One possible mechanism of the hTERT effect on EPC differentiation may involve delay in senescence related to cell culture shock.[35] Aging is one of the factors that might affect senescence; eg, EPCs from older people might go into senescence more rapidly than do EPCs used in the current experiments. Further investigation concerning time course in EPC senescence should be necessary. The in vivo experiments described here may be interpreted to constitute proof of concept that indirect gene transfer may facilitate therapeutic applications of EPC transplantation. The dose of EPCs used in the current in vivo experiments was 30× less than that required in previous experiments designed to improve the rate of limb salvage.[7] Moreover, GFP overexpression did not affect on EPC functions because of the equivalent finding of GFP-transduced EPCs and nontransduced EPCs with cell senescence and migratory and mitogenic activities. Thus, Td/hTERT EPC gene transfer constitutes one option to address the relative paucity of EPCs that can be isolated from peripheral blood before ex vivo expansion and subsequent autologous readministration.

We have questioned if hTERT-expressing cells acquired characteristics of cancer cells, such as chromosomal abnormalities, anchorage-independent growth in culture, or tumorigenicity in immunodeficient mice. There was no observation of such neoplasticity, however, after hTERT transduction by adenovirus constructs. The ectopic hTERT expression by adenovirus transduction was limited within 4 weeks and did not bring immortalization on EPCs. The stability of endothelial lineage cell after hTERT overexpression was also supported by the findings that hTERT-transduced differentiated ECs exhibited neither evidence of malignant transformation nor loss of functional and morphogenetic characteristics of the parental cells.[22] We are paying attention to every possibility for applying this approach to any experimental or clinical application.

The augmented neovascularization observed after therapeutic transplantation of hTERT overexpressing EPCs is consistent with the favorable impact of hTERT gene transfer on the angiogenic profiles of EPCs in the in vitro experiments. As foci of injured organs are exposed to diverse physiological and pathological stress, replication and differentiation of certain cells (particularly stem and/or progenitor cells) may be required to initiate and complete tissue regeneration. The concept of "rejuvenating" EPCs via delay in senescence and enhanced regenerative properties may thus have therapeutic implications for vascular disorders, including myocardial ischemia and lower extremity, in which the viability of these and fully differentiated ECs is recurrently subjected to a variety of individual and environmental stress factors.

## Acknowledgments

This work was supported by grants from the National Institutes of Health, the Peter Lewis Foundation, and the American Heart Association. Dr Asahara is supported in part by New Energy and Industrial Technology Development Organization. Dr Murasawa is a recipient of a grant from the Japan Society for the Promotion of Science (JSPS) Postdoctoral Fellowships for Research Abroad.

## References

1. Asahara T, Murohara T, Sullivan A, et al. Isolation of putative progenitor endothelial cells for angiogenesis. *Science*. 1997;275:964–967.
2. Shi Q, Rafii S, Wu MH, et al. Evidence for circulating bone marrow-derived endothelial cells. *Blood*. 1998;92:362–367.
3. Asahara T, Masuda H, Takahashi T, et al. Bone marrow origin of endothelial progenitor cells responsible for postnatal vasculogenesis in physiological and pathological neovascularization. *Circ Res*. 1999;85:221–228.
4. Takahashi T, Kalka C, Masuda H, et al. Ischemia- and cytokine-induced mobilization of bone marrow–derived endothelial progenitor cells for neovascularization. *Nat Med*. 1999;5:434–438.

5. Gunsilius E, Duba HC, Petzer AL, et al. Evidence from a leukaemia model for maintenance of vascular endothelium by bone marrow-derived endothelial cells. *Lancet.* 2000;355:1688–1691.
6. Kawamoto A, Gwon HC, Iwaguro H, et al. Therapeutic potential of ex vivo expanded endothelial progenitor cells for myocardial ischemia. *Circulation.* 2001;103:634–637.
7. Kalka C, Masuda H, Takahashi T, et al. Transplantation of ex vivo expanded endothelial progenitor cells for therapeutic neovascularization. *Proc Natl Acad Sci U S A.* 2000;97:3422–3427.
8. Iwaguro H, Yamaguchi J, Kalka C, et al. Endothelial progenitor cell vascular endothelial growth factor gene transfer for vascular regeneration. *Circulation.* 2002;105:732–738.
9. Harley CB, Futcher AB, Greider CW. Telomeres shorten during ageing of human fibroblasts. *Nature.* 1990;345:458–460.
10. Hastie ND, Dempster M, Dunlop MG, et al. Telomere reduction in human colorectal carcinoma and with ageing. *Nature.* 1990;346:866–868.
11. Wright WE, Shay JW. The two-stage mechanism controlling cellular senescence and immortalization. *Exp Gerontol.* 1992;27:383–389.
12. Greider CW. Telomeres, telomerase and senescence. *Bioessays.* 1990;12: 363–369.
13. Nakamura TM, Morin GB, Chapman KB, et al. Telomerase catalytic subunit homologs from fission yeast and human. *Science.* 1997;277: 955–959.
14. Harrington L, Zhou W, McPhail T, et al. Human telomerase contains evolutionarily conserved catalytic and structural subunits. *Genes Dev.* 1997;11:3109–3115.
15. Kilian A, Bowtell DD, Abud HE, et al. Isolation of a candidate human telomerase catalytic subunit gene, which reveals complex splicing patterns in different cell types. *Hum Mol Genet.* 1997;6:2011–2019.
16. Meyerson M, Counter CM, Eaton EN, et al. hEST2, the putative human telomerase catalytic subunit gene, is up-regulated in tumor cells and during immortalization. *Cell.* 1997;90:785–795.
17. Kolquist KA, Ellisen LW, Counter CM, et al. Expression of TERT in early premalignant lesions and a subset of cells in normal tissues. *Nat Genet.* 1998;19:182–186.
18. Hayflick L, Moorhead P. The serial cultivation of human diploid strains. *Exp Cell Res.* 1961;25:585–621.
19. Bodnar AG, Ouellette M, Frolkis M, et al. Extension of life-span by introduction of telomerase into normal human cells. *Science.* 1998;279: 349–352.
20. Jiang XR, Jimenez G, Chang E, et al. Telomerase expression in human somatic cells does not induce changes associated with a transformed phenotype. *Nat Genet.* 1999;21:111–114.
21. Morales CP, Holt SE, Ouellette M, et al. Absence of cancer-associated changes in human fibroblasts immortalized with telomerase. *Nat Genet.* 1999;21:115–118.
22. Yang J, Chang E, Cherry AM, et al. Human endothelial cell life extension by telomerase expression. *J Biol Chem.* 1999;274:26141–26148.
23. Matsushita H, Chang E, Glassford AJ, et al. eNOS activity is reduced in senescent human endothelial cells: preservation by hTERT immortalization. *Circ Res.* 2001;89:793–798.
24. Asahara T, Takahashi T, Masuda H, et al. VEGF contributes to postnatal neovascularization by mobilizing bone marrow-derived endothelial progenitor cells. *EMBO J.* 1999;18:3964–3972.
25. He TC, Zhou S, da Costa LT, et al. A simplified system for generating recombinant adenoviruses. *Proc Natl Acad Sci U S A.* 1998;95: 2509–2514.
26. Miyake S, Makimura M, Kanegae Y, et al. Efficient generation of recombinant adenoviruses using adenovirus DNA-terminal protein complex and a cosmid bearing the full-length virus genome. *Proc Natl Acad Sci U S A.* 1996;93:1320–1324.
27. Vasa M, Breitschopf K, Zeiher AM, et al. Nitric oxide activates telomerase and delays endothelial cell senescence. *Circ Res.* 2000;87: 540–542.
28. Kureishi Y, Luo Z, Shiojima I, et al. The HMG-CoA reductase inhibitor simvastatin activates the protein kinase Akt and promotes angiogenesis in normocholesterolemic animals. *Nat Med.* 2000;6:1004–1010.
29. Couffinhal T, Silver M, Zheng LP, et al. Mouse model of angiogenesis. *Am J Pathol.* 1998;152:1667–1679.
30. Murohara T, Asahara T, Silver M, et al. Nitric oxide synthase modulates angiogenesis in response to tissue ischemia. *J Clin Invest.* 1998;101: 2567–2578.
31. Rivard A, Silver M, Chen D, et al. Rescue of diabetes-related impairment of angiogenesis by intramuscular gene therapy with adeno-VEGF. *Am J Pathol.* 1999;154:355–363.
32. Wardell K, Jakobsson A, Nilsson GE. Laser Doppler perfusion imaging by dynamic light scattering. *IEEE Trans Biomed Eng.* 1993;40:309–316.
33. Linden M, Sirsjo A, Lindbom L, et al. Laser-Doppler perfusion imaging of microvascular blood flow in rabbit tenuissimus muscle. *Am J Physiol.* 1995;269:H1496–H1500.
34. Couffinhal T, Silver M, Kearney M, et al. Impaired collateral vessel development associated with reduced expression of vascular endothelial growth factor in $ApoE^{-/-}$ mice. *Circulation.* 1999;99:3188–3198.
35. Sherr CJ, DePinho RA. Cellular senescence: mitotic clock or culture shock? *Cell.* 2000;102:407–410.

# Extension of Life-Span by Introduction of Telomerase into Normal Human Cells

Andrea G. Bodnar,* Michel Ouellette,* Maria Frolkis, Shawn E. Holt, Choy-Pik Chiu, Gregg B. Morin, Calvin B. Harley, Jerry W. Shay, Serge Lichtsteiner,† Woodring E. Wright†

Normal human cells undergo a finite number of cell divisions and ultimately enter a nondividing state called replicative senescence. It has been proposed that telomere shortening is the molecular clock that triggers senescence. To test this hypothesis, two telomerase-negative normal human cell types, retinal pigment epithelial cells and foreskin fibroblasts, were transfected with vectors encoding the human telomerase catalytic subunit. In contrast to telomerase-negative control clones, which exhibited telomere shortening and senescence, telomerase-expressing clones had elongated telomeres, divided vigorously, and showed reduced staining for β-galactosidase, a biomarker for senescence. Notably, the telomerase-expressing clones have a normal karyotype and have already exceeded their normal life-span by at least 20 doublings, thus establishing a causal relationship between telomere shortening and in vitro cellular senescence. The ability to maintain normal human cells in a phenotypically youthful state could have important applications in research and medicine.

Normal human diploid cells placed in culture have a finite proliferative life-span and enter a nondividing state termed senescence, which is characterized by altered gene expression (*1*, *2*). Replicative senescence is dependent upon cumulative cell divisions and not chronologic or metabolic time, indicating that proliferation is limited by a "mitotic clock" (*3*). The reduction in proliferative capacity of cells from old donors and patients with premature aging syndromes (*4*), and the accumulation in vivo of senescent cells with altered patterns of gene expression (*5*, *6*), implicate cellular senescence in aging and age-related pathologies (*1*, *2*).

Telomere loss is thought to control entry into senescence (*7*–*10*). Human telomeres consist of repeats of the sequence TTAGGG/CCCTAA at chromosome ends; these repeats are synthesized by the ribonucleoprotein enzyme telomerase (*11*, *12*). Telomerase is active in germline cells and, in humans, telomeres in these cells are maintained at about 15 kilobase pairs (kbp). In contrast, telomerase is not expressed in most human somatic tissues (*13*, *14*), and telomere length is significantly shorter (*15*). The telomere hypothesis of cellular aging (*16*) proposes that cells become senescent when progressive telomere shortening during each division produces a threshold telomere length.

The human telomerase reverse transcriptase subunit (hTRT) has been cloned (*17*). We recently demonstrated that telomerase activity can be reconstituted by transient expression of hTRT in normal human diploid cells, which express low levels of the template RNA component of telomerase (hTR) but do not express hTRT (*18*). This provided the opportunity to manipulate telomere length and test the hypothesis that telomere shortening causes cellular senescence.

**Introduction of telomerase into normal human cells.** To determine if telomerase expression increases cell life-span, we transfected hTRT$^-$ normal cells with two different hTRT expression constructs. One construct was engineered for increased translational efficiency by removal of the 5′ and 3′ untranslated regions of hTRT and creation of a Kozak consensus sequence. This engineered hTRT cDNA was cloned downstream of the MPSV promoter (*19*). The second construct consisted of the complete (native) hTRT cDNA cloned downstream of the SV40 promoter in pZeoSV (*19*). In the first experiments, we compared the life-span of stable clones transfected with MPSV-hTRT versus "vector only" clones, and in the second, we compared the life-span of activity-positive and activity-negative stable clones containing integrated SV40-hTRT constructs.

hTRT$^-$ normal retinal pigment epithelial cells (RPE-340) were transfected with the MPSV-hTRT vector at population doubling (PD) 37, and 27 of the 39 resultant stable clones (69%) expressed telomerase activity. BJ foreskin fibroblasts were transfected with the MPSV-hTRT vector at PD 58, and 3 of the 22 stable clones (14%) expressed telomerase activity. Reverse transcriptase–polymerase chain reaction experiments demonstrated that the hTRT mRNA originated from the transfected cDNA and not the endogenous gene (*20*). Telomerase activity, measured relative to that in the lung cancer–derived human cell line H1299, ranged from 65 to 360% in the RPE clones (Fig. 1) and 86 to 95% in the BJ clones. This range of telomerase activity is similar to that observed for tumor cell lines (*13*). Thirty-three RPE clones and 24 BJ clones transfected with the control plasmid were also isolated; RPE clones that generated sufficient cells for the TRAP assay ($n$ = 15) (Fig. 1) and control BJ clones ($n$ = 15)

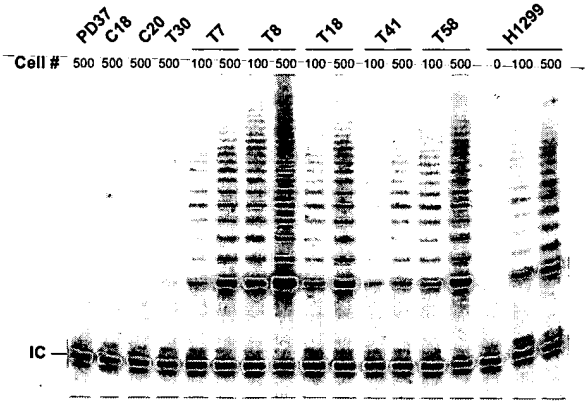


**Fig. 1.** Telomerase activity in stable RPE clones. Stable human RPE clones obtained by transfection with a control vector (clone numbers prefixed with "C") or with a vector expressing the hTRT cDNA ("T" clones) were analyzed for telomerase activity by the TRAP assay (*19*). "PD37" represents the cell population at the time of transfection. The number of cells assayed for each clone is indicated above each lane. "IC" is the internal control in the TRAP assay. The positive control was the telomerase activity extracted from H1299 cells (*20*).

A. G. Bodnar, M. Frolkis, C.-P. Chiu, G. B. Morin, C. B. Harley, and S. Lichtsteiner are at Geron Corporation, 230 Constitution Drive, Menlo Park, CA 94025, USA. M. Ouellette, S. E. Holt, J. W. Shay, and W. E. Wright are in the Department of Cell Biology and Neuroscience, University of Texas Southwestern Medical Center, 5323 Harry Hines Boulevard, Dallas, TX 75235–9039, USA.

*These authors contributed equally to this work.
†To whom correspondence should be addressed. E-mail: slichtste@geron.com; wright@utsw.swmed.edu

were negative for telomerase activity. BJ fibroblasts were also transfected with the pZeoSV-hTRT construct at PD 44. Six of 76 clones (8%) expressed telomerase activity ranging from 10 to 30% of that in the reference H1299 cell line. As assessed by a ribonuclease protection assay, hTRT mRNA was undetectable in activity-negative BJ cells but readily observed in $hTRT^+$ clones (*20*).

**Telomere lengthening in $hTRT^+$ normal cells.** We then measured telomere lengths to determine if the hTRT-reconstituted telomerase acts on its normal chromosomal substrate (*21*). Telomeres in the $hTRT^-$ cells decreased by 0.4 to 1.3 kbp (Fig. 2), comparable to the shortening seen in mass cultures at equivalent PDs, whereas telomeres in the $hTRT^+$ RPE and BJ clones transfected with the MPSV-hTRT vector increased by 3.7 kbp (± 1.4 kbp, $n = 26$) and 7.1 kbp (± 0.3 kbp, $n = 3$), respectively. Telomeres in six $hTRT^+$ clones transfected with the pZeoSV-hTRT vector, increased by 0.4 kbp (± 0.3 kbp, $n = 6$). Because two $hTRT^+$ clones expressing only 5 to 7% relative telomerase activity (RPE clone T30 and BJ clone B13) did not maintain telomere length, they were considered to be functionally $hTRT^-$ (Fig. 2B). These results demonstrate that hTRT-reconstituted telomerase extends the endogenous telomeres in a normal cell.

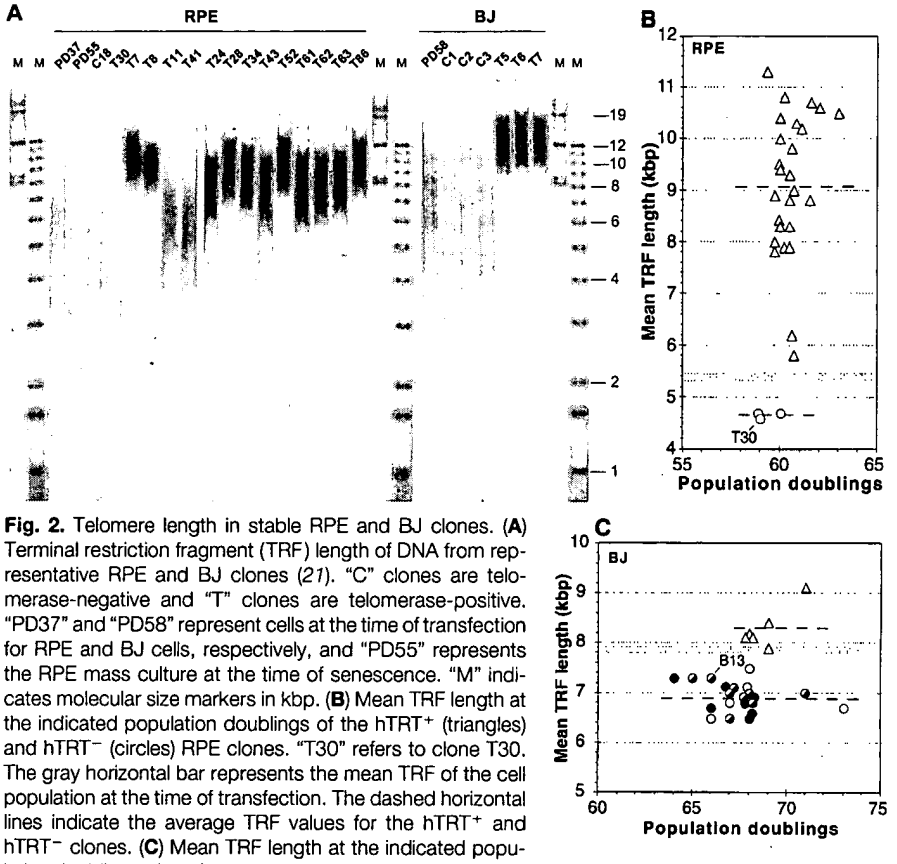


**Fig. 2.** Telomere length in stable RPE and BJ clones. (**A**) Terminal restriction fragment (TRF) length of DNA from representative RPE and BJ clones (*21*). "C" clones are telomerase-negative and "T" clones are telomerase-positive. "PD37" and "PD58" represent cells at the time of transfection for RPE and BJ cells, respectively, and "PD55" represents the RPE mass culture at the time of senescence. "M" indicates molecular size markers in kbp. (**B**) Mean TRF length at the indicated population doublings of the $hTRT^+$ (triangles) and $hTRT^-$ (circles) RPE clones. "T30" refers to clone T30. The gray horizontal bar represents the mean TRF of the cell population at the time of transfection. The dashed horizontal lines indicate the average TRF values for the $hTRT^+$ and $hTRT^-$ clones. (**C**) Mean TRF length at the indicated population doublings of the BJ clones transfected with pZeoSV-hTRT; designations are as in (B). "B13" refers to clone B13. Closed symbols represent cells that senesced; half-filled symbols correspond to cells near senescence (dividing less than once per week).

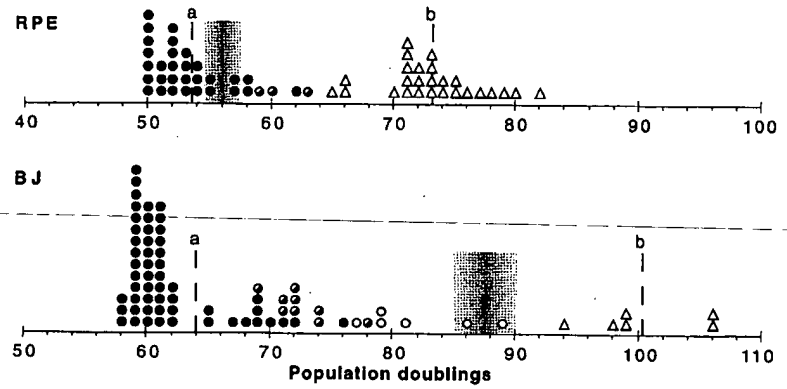


**Fig. 3.** Effect of telomerase expression on cell life-span. The proliferative status of each RPE (upper panel) and BJ (lower panel; pZeoSV-hTRT experiment) clone is shown. The $hTRT^+$ clones (triangles) and the $hTRT^-$ clones (circles) are plotted (*35*). Closed symbols represent senescent clones (dividing less than once per 2 weeks); half-filled symbols correspond to cells near senescence (dividing less than once per week); open symbols represent clones dividing more than once per week. The shaded vertical area indicates the typical PD range where the mass population of cells senesce. Dashed vertical lines represent the mean PD of: (a) the $hTRT^-$ and (b) the $hTRT^+$ clones.

**Life-span, karyotype, and phenotype.** To investigate the effect of telomerase expression on the life-span of normal cells, we compared the growth of $hTRT^+$ and $hTRT^-$ clones. $hTRT^-$ RPE clones showed the expected slowing of growth that is associated with aging in vitro, and 30 out of 33 senesced (*22*) by an age typical for mass RPE cultures (Fig. 3). In contrast, $hTRT^+$ RPE clones transfected with MPSV-hTRT exceeded the mean life-span of the $hTRT^-$ clones by ~20 doublings ($P < 10^{-24}$; Student's $T$ test). These clones have exceeded the maximal RPE life-span (PD 55 to 57), and continue to divide at the rate of young RPEs (Fig. 3). Similarly, most of the $hTRT^-$ BJ fibroblast clones senesced or are near senescent (64 of 70 clones), whereas all six of the $hTRT^+$ clones transfected with the pZeoSV-hTRT vector exceeded the maximal BJ life-span (85 to 90 PD) (Fig. 3). The average PD of these six rapidly dividing $hTRT^+$ clones is already 36 doublings beyond the average life-span of the 70 $hTRT^-$ clones ($P < 10^{-6}$). Similar results were obtained with human vascular endothelial cells (*23*). Thus, expression of functional hTRT in normal cells extends their life-span.

Senescence-associated β-galactosidase (SA–β-Gal) is an established biomarker associated with cellular aging (*6*). We stained $hTRT^-$ RPE clones at or near senescence and compared the level of SA–β-Gal staining to that in $hTRT^+$ clones that had undergone a similar or greater number of cell divisions (Fig. 4, A and B). A majority of the cells in the $hTRT^-$ clones showed strong staining; by contrast, few of the cells in $hTRT^+$ clones at equivalent or greater PD showed staining. The cells of the $hTRT^-$ clones that had stopped dividing exhibited SA–β-Gal staining levels equivalent to that observed in senescent mass

cultures. Their large size and increased ratio of cytoplasm:nucleus also indicates that the clones had senesced (Fig. 4A). The remainder of the slowly dividing hTRT$^-$ clones exhibited SA–β-Gal staining typical of cells close to senescence. The same result was found for fibroblasts: Six of six hTRT$^+$ clones showed low levels of staining typical of young fibroblast cultures, whereas all of the hTRT$^-$ clones showed elevated SA–β-Gal staining (Fig. 4C). Detailed G-banding of two hTRT$^+$ RPE clones and two hTRT$^+$ BJ clones revealed that the cells had the normal complement of 46 chromosomes and no abnormalities (*24*). hTRT$^+$ cells with an extended life-span therefore appear to have a normal karyotype and phenotype similar to young cells.

**Implications.** Our results indicate that telomere loss in the absence of telomerase is the intrinsic timing mechanism that controls the number of cell divisions prior to senescence. The long-term effects of exogenous telomerase expression on telomere maintenance and the life-span of these cells remain to be determined in studies of longer duration.

Telomere homeostasis is likely to result from a balance of lengthening and shortening activities. Although certain proteins in yeast are thought to facilitate the interaction of telomerase with the telomere (*25*), our results indicate that if analogous mammalian factors are required, they are already present in hTRT$^-$ human cells. The telomerase catalytic subunit produces the lengthening activity, but other factors including telomere binding proteins such as hTRF-1 and -2 (*26*) might be involved in establishing a telomere length equilibrium. Very low levels of telomerase activity, such as that exhibited by RPE clone T30 and BJ clone B13, are apparently insufficient to prevent telomere shortening. This is consistent with the observation that stem cells have low but detectable telomerase activity, yet continue to exhibit shortening of their telomeres throughout life (*27*). Thus, we believe that a threshold level of telomerase activity is required for life-span extension. Promoter strength, structure of untranslated regions, site of integration, levels of hTR and hTRT, and telomere- or telomerase-associated proteins in specific cell types are all factors that may affect the functional level of telomerase. This hypothesis is supported by our finding that hTRT$^+$ clones derived from different cell types and transfected with different vectors showed marked differences in telomere lengths.

Certain stem cells or germline populations are telomerase positive (*13*, *27*, *28*) and have long or indefinite life-spans, illustrating that telomerase expression per se is not oncogenic. Cellular transformation with viral oncoproteins can also extend cell life-span, but through mechanisms that reduce checkpoint control, increase genomic instability, and fail to prevent telomere loss (*29*, *30*). We have not observed any gross phenotypic or morphological characteristics of transformed cells (such as loss of contact inhibition or growth in low serum) that might account for the extended proliferative capacity of the hTRT$^+$ cells. The normal karyotype and the absolute correlation between extended life-span and telomerase activity suggest that stochastic mutagenesis does not account for the life-span extension.

Cellular senescence is believed to contribute to multiple conditions in the elderly

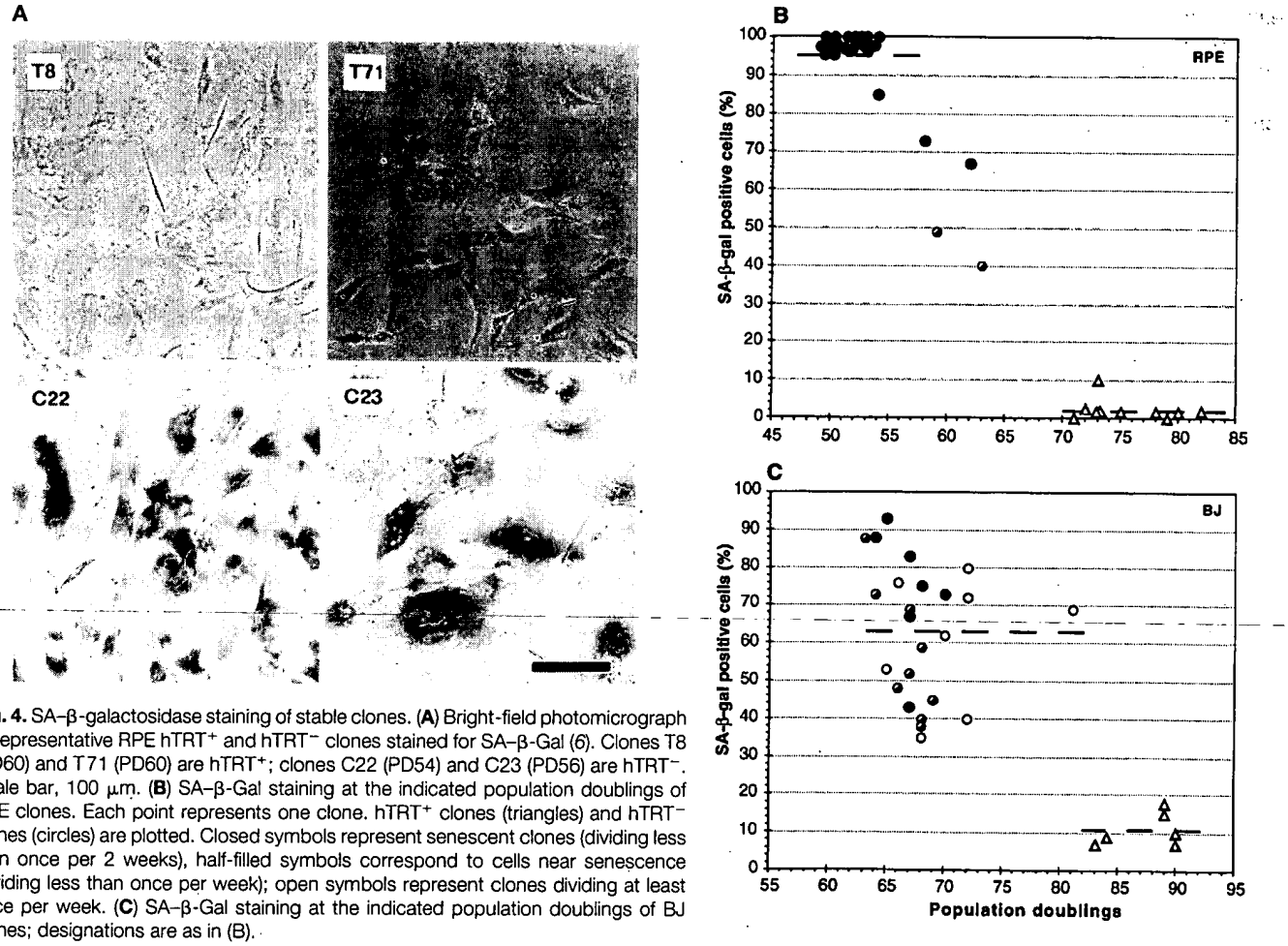


**Fig. 4.** SA–β-galactosidase staining of stable clones. (**A**) Bright-field photomicrograph of representative RPE hTRT$^+$ and hTRT$^-$ clones stained for SA–β-Gal (*6*). Clones T8 (PD60) and T71 (PD60) are hTRT$^+$; clones C22 (PD54) and C23 (PD56) are hTRT$^-$. Scale bar, 100 μm. (**B**) SA–β-Gal staining at the indicated population doublings of RPE clones. Each point represents one clone. hTRT$^+$ clones (triangles) and hTRT$^-$ clones (circles) are plotted. Closed symbols represent senescent clones (dividing less than once per 2 weeks), half-filled symbols correspond to cells near senescence (dividing less than once per week); open symbols represent clones dividing at least once per week. (**C**) SA–β-Gal staining at the indicated population doublings of BJ clones; designations are as in (B).

that could in principle be remedied by cell life-span extension in situ. Examples include atrophy of the skin through loss of extracellular matrix homeostasis in dermal fibroblasts (*31*); age-related macular degeneration caused by accumulation of lipofuscin and downregulation of a neuronal survival factor in RPE cells (*32*); and atherosclerosis caused by loss of proliferative capacity and overexpression of hypertensive and thrombotic factors in endothelial cells (*9*, *33*). Extended life-span cells also have potential applications ex vivo. Cloned normal diploid cells could replace established tumor cell lines in studies of biochemical and physiological aspects of growth and differentiation; long-lived normal human cells could be used for the production of normal or engineered biotechnology products; and expanded populations of normal or genetically engineered rejuvenated cells could be used for autologous or allogeneic cell and gene therapy. Thus the ability to extend cellular life-span, while maintaining the diploid status, growth characteristics, and gene expression pattern typical of young normal cells, has important implications for biological research, the pharmaceutical industry, and medicine.

*Note added in proof:* As of the time of galley proofs, virtually all of the hTRT$^-$ clones were senescent or near senescent, whereas all of the hTRT$^+$ clones continued to divide rapidly.

## REFERENCES AND NOTES


1. L. Hayflick and P. S. Moorhead, *Exp. Cell Res.* **25**, 585 (1961); W. E. Wright, O. M. Periera-Smith, J. W. Shay, *Mol. Cell. Biol.* **9**, 3088 (1989); S. Goldstein, *Science* **249**, 1129 (1990).
2. J. Campisi, *Cell* **84**, 497 (1996); J. Campisi, *Eur. J. Cancer* **33**, 703 (1997); R. G. A. Faragher and S. Shall, *Drug Discovery Today* **2**, 64 (1997).
3. R. T. Dell'Orco, J. G. Mertens, P. F. J. Kruse, *Exp. Cell Res.* **77**, 356 (1973); C. B. Harley and S. Goldstein, *J. Cell. Physiol.* **97**, 509 (1978).
4. G. M. Martin, C. A. Sprague, C. J. Epstein, *Lab. Invest.* **23**, 86 (1970); E. L. Schneider and Y. Mitsui, *Proc. Natl. Acad. Sci. U.S.A.* **73**, 3584 (1976); E. L. Schneider and C. J. Epstein, *Proc. Soc. Exp. Biol. Med.* **141**, 1092 (1972); E. Elmore and M. Swift, *J. Cell Physiol.* **87**, 229 (1976).
5. B. M. Stanulis-Praeger, *Mech. Ageing Dev.* **38**, 1 (1987).
6. G. P. Dimri *et al.*, *Proc. Natl. Acad. Sci. U.S.A.* **92**, 9363 (1995).
7. C. B. Harley, A. B. Futcher, C. W. Greider, *Nature* **345**, 458 (1990); R. C. Allsopp *et al.*, *Proc. Natl. Acad. Sci. U.S.A.* **89**, 10114 (1992); H. Vaziri *et al.*, *Am. J. Hum. Genet.* **52**, 661 (1993).
8. N. D. Hastie *et al.*, *Nature* **346**, 866 (1990); W. E. Wright and J. W. Shay, *Exp. Gerontol.* **27**, 383 (1992); W. E. Wright and J. W. Shay, *Trends Cell Biol.* **5**, 293 (1995); R. B. Effros *et al.*, *AIDS* **10**, F17 (1996); D. Wynford-Thomas, *Oncology Res.* **8**, 387 (1996).
9. E. Chang and C. B. Harley, *Proc. Natl. Acad. Sci. U.S.A.* **92**, 11190 (1995).
10. N.-P. Weng, B. L. Levine, C. H. June, R. J. Hodes, *Proc. Natl. Acad. Sci. U.S.A.* **92**, 11091 (1995).
11. J. Lingner *et al.*, *Science* **276**, 561 (1997).
12. C. W. Greider and E. H. Blackburn *Nature* **337**, 331 (1989); J. Feng *et al.*, *Science* **269**, 1236 (1995).
13. N. W. Kim *et al.*, *Science* **266**, 2011 (1994).
14. J. W. Shay and S. Bacchetti, *Eur. J. Cancer* **33**, 777 (1997).
15. H. J. Cooke and B. A. Smith, *Cold Spring Harb. Lab. Symp. Quant. Biol.* **51**, 213 (1986); T. de Lange *et al.*, *Mol. Cell Biol.* **10**, 518 (1990).
16. C. B. Harley, *Mutat. Res.* **256**, 271 (1991).
17. T. M. Nakamura *et al.*, *Science* **277**, 955 (1997); M. Meyerson *et al.*, *Cell* **90**, 78 (1997); A. Kilian *et al.*, *Hum. Mol. Genet.* **6**, 2011 (1997).
18. S. L. Weinrich *et al.*, *Nature Genet.* **17**, 498 (1997).
19. RPE-340 cells and BJ fibroblasts were cultured as previously described (*18*). In one set of experiments, RPE and BJ cells were subjected to electroporation with control vector (pBBS212) or vector encoding hTRT with a consensus Kozak sequence downstream of the myeloproliferative sarcoma virus (MPSV) promoter (pGRN145) (*18*). After 48 hours, transfected cells were placed into medium containing Hygromycin-B (50 μg/ml) for 2 to 3 weeks, at which time the concentration was reduced to 10 μg/ml. Individual stable clones were selected and analyzed for telomerase activity by the telomeric repeat amplification protocol (TRAP) (*13*, *18*). In a separate experiment, BJ fibroblasts were transfected with pZeoSV-hTRT, a derivative of pZeoSV (Invitrogen, Carlsbad, CA) encoding hTRT downstream of the simian virus 40 (SV40) promoter. After electroporation, the BJ cells were cultured in zeocin (200 μg/ml). hTRT$^+$ and hTRT$^-$ clones from each transfection were obtained and expanded.
20. Reverse transcriptase–polymerase chain reaction (RT-PCR) was performed on cells transfected with pGRN145. Endogenous hTRT mRNA was detected with the primer set RA58 (5′-GGCTGAAGTGTCACAG-3′) and hTRT3′UTR (5′-GGCTGCTGGTGTCTGCTCTCGGCC-3′). Exogenous hTRT mRNA was detected with the primer set RA58 and RA55 (5′-TCCGCACGTGAGAAT-3′). RT-PCR showed that the hTRT mRNA derived from the transfected cDNA, but not the endogenous hTRT mRNA, was present in telomerase-positive RPE ($n$ = 4) and BJ ($n$ = 3) clones (*34*). Ribonuclease protection assays were performed on BJ cells transfected with pZeoSV-hTRT and on H1299 cells (NCI-H1299, American Type Culture Collection). The probe corresponded to hTRT sequences spanning amino acids 541 to 647. The abundance of the catalytic subunit was comparable to that in H1299 cells (*34*).
21. DNA isolation and TRF analyses for the RPE and BJ clones were performed essentially as described (*7*), except that in some cases the DNA was resolved on 0.6% agarose gels and electroblotted to nylon membranes (*18*), and for mean TRF calculations, the average of the weighted and unweighted means was used [M. Levy, R. C. Allsopp, A. B. Futcher, C. W. Greider, C. B. Harley, *J. Mol. Biol.* **225**, 951 (1992)].
22. Senescence is defined as less than one PD in 2 weeks; near-senescence is defined as less than one PD per week. Young BJ and RPE cells typically double in 1 to 2 days.
23. A. G. Bodnar *et al.*, unpublished data.
24. Chromosomes were analyzed by G-banding with trypsin and Wright's stain (GTW) by the Clinical Cytogenetics Laboratory, Stanford Health Services (RPE clones) and the Cytogenetics Laboratory, University of Texas Southwestern Medical Center (BJ clones).
25. L. M. C. Konkel *et al.*, *Proc. Natl. Acad. Sci. U.S.A.* **92**, 5558 (1995); P. W. Greenwell *et al.*, *Cell* **82**, 823 (1995); T. Lendvay, D. Morris, J. Sah, B. Balasubramanian, V. Lundblad, *Genetics* **144**, 1399 (1996); D. Wotton and D. Shore, *Genes Dev.* **11**, 748 (1997); S. Marcand, E. Gilson, D. Shore, *Science* **275**, 986 (1997).
26. D. Broccoli, A. Smogorzewska, L. Chong, T. de Lange, *Nature Genet.* **17**, 231 (1997); B. van Steensel and T. de Lange, *Nature* **385**, 740 (1997).
27. C.-P. Chiu *et al.*, *Stem Cells* **14**, 239 (1996).
28. A. Bodnar, N. W. Kim, R. B. Effros, C.-P. Chiu, *Exp. Cell Res.* **228**, 58 (1996); W. E. Wright, M. A. Piatyszek, W. E. Rainey, W. Byrd, J. W. Shay, *Dev. Genet.* **18**, 173 (1996); M. Engelhardt *et al.*, *Blood* **90**, 182 (1997).
29. C. M. Counter *et al.*, *EMBO J.* **11**, 1921 (1992); J. W. Shay, W. E. Wright, H. Werbin, *Int. J. Oncol.* **3**, 559 (1993); J. W. Shay, W. E. Wright, D. Brasiskyte, B. A. Van Der Haegen, *Oncogene* **8**, 1407 (1993); J. W. Shay, B. A. Van der Haegen, Y. Ying, W. E. Wright, *Exp. Cell Res.* **209**, 45 (1993).
30. J. W. Shay, O. M. Pereira-Smith, W. E. Wright, *Exp. Cell Res.* **196**, 33 (1991).
31. K. Takeda, A. Gosiewska, B. Peterkofsky, *J. Cell. Physiol.* **153**, 450 (1992); M. D. West, *Arch. Dermatol.* **130**, 87 (1994).
32. M. Boulton, F. Docchio, P. Dayhaw-Barker, R. Ramponi, R. Cubeddu, *Vision Res.* **30**, 1291 (1990); J. Tombran-Tink, S. M. Shivaram, G. J. Chader, L. V. Johnson, D. Bok, *J. Neurosci.* **15**, 4992 (1995).
33. T. Kumazaki, *Hiroshima J. Med. Sci.* **42**, 97 (1993).
34. S. Lichtsteiner, I. Savre-Train, M. Ouellette, unpublished results.
35. To accumulate doublings as rapidly as possible, we shifted all six hTRT$^+$ BJ clones and the six fastest growing hTRT$^-$ BJ clones from 10% to 20% serum and maintained them in continuous log growth as of PD 66 to 78 (hTRT$^-$) or PD 74 to 80 (hTRT$^+$). Neither increased serum nor exponential growth conditions significantly extends life-span [T. Ohno, *Mech. Ageing Devel.* **11**, 179 (1979); J. R. Smith and K. I. Braunschweiger, *J. Cell Physiol.* **98**, 597 (1979)] particularly if instituted near the proliferative limit of the culture.


36. We thank M. Liao, J.-F. Train, V. Tesmer, B. Frank, Y. Oei, S. Gitin, S. Wong, V. Votin, B. Lastelic, R. Adams, S. Amshey, D. Choi, and N. Spiff-Robinson for excellent technical assistance; W. Andrews and R. Adams for the construction of the MPSV vector; L. Hjelmeland for the RPE-340 cells; J. Smith for the BJ fibroblasts; M. Kozlowski for helpful discussions; L. Hayflick and T. R. Cech for critical reading of the manuscript; I. Savre-Train for the ribonuclease protection results; and W. O'Wheels for support during manuscript preparation. Supported in part by NIH grant AG07992 (W.E.W.) and NIH postdoctoral fellowship AG05747 (S.E.H.).

1 December 1997; accepted 22 December 1997